Article

Synthesis and X-ray or NMR/DFT Structure Elucidation of Twenty-One New Trifluoromethyl Derivatives of Soluble Cage Isomers of C, C, C, and C

Ivan E. Kareev, Alexey A. Popov, Igor V. Kuvychko, Natalia B. Shustova, Sergey F. Lebedkin, Vyachevslav P. Bubnov, Oren P. Anderson, Konrad Seppelt, Steven H. Strauss, and Olga V. Boltalina

J. Am. Chem. Soc., **2008**, 130 (40), 13471-13489 • DOI: 10.1021/ja8041614 • Publication Date (Web): 13 September 2008

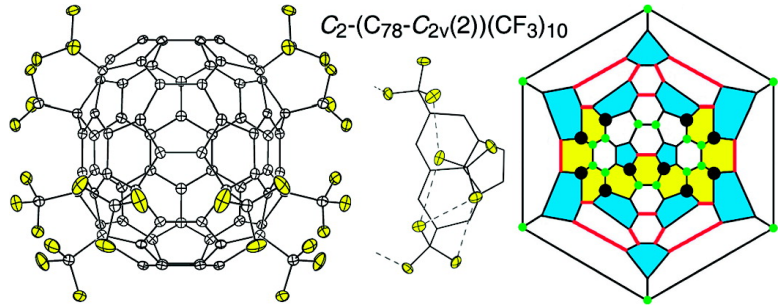

More About This Article

Additional resources and features associated with this article are available within the HTML version:

- Supporting Information
- Links to the 1 articles that cite this article, as of the time of this article download
- Access to high resolution figures
- Links to articles and content related to this article
- Copyright permission to reproduce figures and/or text from this article

View the Full Text HTML

J|A|C|S
ARTICLES

Published on Web 09/13/2008

Synthesis and X-ray or NMR/DFT Structure Elucidation of Twenty-One New Trifluoromethyl Derivatives of Soluble Cage Isomers of C_{76}, C_{78}, C_{84}, and C_{90}

Ivan E. Kareev,*,†,§ Alexey A. Popov,*,‡ Igor V. Kuvychko,¶ Natalia B. Shustova,¶ Sergey F. Lebedkin,§ Vyachevslav P. Bubnov,† Oren P. Anderson,¶ Konrad Seppelt,# Steven H. Strauss,*,¶ and Olga V. Boltalina*,¶

Department of Chemistry, Colorado State University, Fort Collins, Colorado 80523, Chemistry Department, Moscow State University, Moscow 119992, Russia, Institute of Problems in Chemical Physics, Russian Academy of Sciences, Chernogolovka 142432, Russia, Institute for Inorganic and Analytical Chemistry, Free University Berlin, D-14195 Berlin, Germany, and Institute for Nanotechnology, Forschungszentrum Karlsruhe, Karlsruhe 76021, Germany

Received June 2, 2008; E-mail: kareev@icp.ac.ru; popov@phys.chem.msu.ru; steven.strauss@colostate.edu; ovbolt@lamar.colostate.edu

Abstract: Adding 1% of the metallic elements cerium, lanthanum, and yttrium to graphite rod electrodes resulted in different amounts of the hollow higher fullerenes (HHFs) C_{76}-D_2(1), C_{78}-C_{2v}(2), and C_{78}-C_{2v}(3) in carbon-arc fullerene-containing soots. The reaction of trifluoroiodomethane with these and other soluble HHFs at 520−550 °C produced 21 new $C_{76,78,84,90}(CF_3)_n$ derivatives (n = 6, 8, 10, 12, 14). The reaction with C_{76}-D_2(1) produced an abundant isomer of C_2-(C_{76}-D_2(1))$(CF_3)_{10}$ plus smaller amounts of an isomer of C_1-(C_{76}-D_2(1))$(CF_3)_6$, two isomers of C_1-(C_{76}-D_2(1))$(CF_3)_8$, four isomers of C_1-(C_{76}-D_2(1))$(CF_3)_{10}$, and one isomer of C_2-(C_{76}-D_2(1))$(CF_3)_{12}$. The reaction with a mixture of C_{78}-D_3(1), C_{78}-C_{2v}(2), and C_{78}-C_{2v}(3) produced the previously reported isomer C_1-(C_{78}-C_{2v}(3))$(CF_3)_{12}$ (characterized by X-ray crystallography in this work) and the following new compounds: C_2-(C_{78}-C_{2v}(3))$(CF_3)_8$; C_2-(C_{78}-D_3(1))$(CF_3)_{10}$ and C_s-(C_{78}-C_{2v}(2))$(CF_3)_{10}$ (both characterized by X-ray crystallography in this work); C_2-(C_{78}-C_{2v}(2))$(CF_3)_{10}$; and C_1-$C_{78}(CF_3)_{14}$ (cage isomer unknown). The reaction of a mixture of soluble higher fullerenes including C_{84} and C_{90} produced the new compounds C_1-$C_{84}(CF_3)_{10}$ (cage isomer unknown), C_1-(C_{84}-C_2(11))$(CF_3)_{12}$ (X-ray structure reported recently), D_2-(C_{84}-D_2(22))$(CF_3)_{12}$, C_2-(C_{84}-D_2(22))$(CF_3)_{12}$, C_1-$C_{84}(CF_3)_{14}$ (cage isomer unknown), C_1-(C_{90}-C_1(32))$(CF_3)_{12}$, and another isomer of C_1-$C_{90}(CF_3)_{12}$ (cage isomer unknown). All compounds were studied by mass spectrometry, ^{19}F NMR spectroscopy, and DFT calculations. An analysis of the addition patterns of these compounds and three other $HHF(X)_n$ compounds with bulky X groups has led to the discovery of the following addition-pattern principle for HHFs: In general, the most pyramidal cage C(sp^2) atoms in the parent HHF, which form the most electron-rich and therefore the most reactive cage C−C bonds as far as 1,2-additions are concerned, are *not* the cage C atoms to which bulky substituents are added. Instead, ribbons of edge-sharing p-$C_6(X)_2$ hexagons, with X groups on less pyramidal cage C atoms, are formed, and the otherwise "most reactive" fullerene double bonds remain intact.

Introduction

As far as the synthesis, isolation, and study of the largest number of well-characterized exohedral fullerene$(X)_n$ compounds is concerned (i.e., with a single type of substituent X), the class of derivatives with X = CF_3 has no parallel. Prior to this report, there were 40 published fullerene$(CF_3)_n$ X-ray structures plus at least 20 other fullerene$(CF_3)_n$ compounds for which the addition patterns were proposed on the basis of spectroscopy and DFT calculations (in some cases the addition pattern is tentative, having been narrowed down to a few "most likely" possibilities[1,2]). These are listed in Table S-1 in the Supporting Information (see also refs 1 and 2 and references therein). No other substituent X (e.g., H, Me, Ph, F, Cl, Br, CRR′) has even one-quarter as many well-characterized derivatives, let alone as many examples of multiple isomers of a given composition. The only fullerene$(X)_n$ compositions with $n > 2$ and more than two isomers are $C_{60}F_{36}$[3] and $C_{78}(C(COOEt)_2)_3$,[4] with three isomers each; $C_{60}(C(COOEt)_2)_3$,[5] with seven isomers; and $C_{60}(c\text{-}C_2H_4N(Me)C_2H_4)_3$, with nine isomers.[6] In contrast, there are three known isomers each for $C_{60}(CF_3)_4$, $C_{60}(CF_3)_{16}$, and $C_{70}(CF_3)_6$; four each for $C_{60}(CF_3)_6$, $C_{60}(CF_3)_{12}$, $C_{70}(CF_3)_{12}$,

† Russian Academy of Sciences.
§ Institute for Nanotechnology.
‡ Moscow State University.
¶ Colorado State University.
# Free University Berlin.

(1) Popov, A. A.; Kareev, I. E.; Shustova, N. B.; Stukalin, E. B.; Lebedkin, S. F.; Seppelt, K.; Strauss, S. H.; Boltalina, O. V.; Dunsch, L. *J. Am. Chem. Soc.* **2007**, *129*, 11551–11568.
(2) Popov, A. A.; Kareev, I. E.; Shustova, N. B.; Lebedkin, S. F.; Strauss, S. H.; Boltalina, O. V.; Dunsch, L. *Chem. Eur. J.* **2008**, *14*, 107–121.
(3) Paolucci, D.; Paolucci, F.; Marcaccio, M.; Carano, M.; Taylor, R. *Chem. Phys. Lett.* **2004**, *400*, 389–393.
(4) Boudon, C.; Gisselbrecht, J. P.; Gross, M.; Herrmann, A.; Ruttimann, M.; Crassous, J.; Cardullo, F.; Echegoyen, L.; Diederich, F. *J. Am. Chem. Soc.* **1998**, *120*, 7860–7868.

and $C_{70}(CF_3)_{14}$; five for $C_{60}(CF_3)_8$; six for $C_{60}(CF_3)_{10}$; and seven for $C_{70}(CF_3)_{10}$.

There are four principal reasons why so many fullerene$(CF_3)_n$ derivatives have been isolated, have had their addition patterns readily determined in most cases, and have been studied by a battery of physicochemical techniques. First, high-temperature reactions of fullerenes and gaseous CF_3I tend to yield a limited number of abundant isomers, and relatively narrow ranges of compositions can be achieved by judicious choice of reaction conditions.[1,2,7−9] This greatly facilitates HPLC purification and leads to the isolation of milligrams or tens of milligrams of compounds that have high compositional and isomeric purity, and high purity is essential for obtaining meaningful spectroscopic and electrochemical results as well as for growing high-quality single crystals for X-ray diffraction. Second, CF_3 groups are sufficiently large that fullerene$(CF_3)_n$ addition patterns with contiguous cage C(sp^3) atoms are rare,[1,2,10,11] and this tendency generally eliminates from serious consideration more than 90% of the addition patterns that are possible for a generic fullerene-$(X)_n$ compound.[12] Third, ^{19}F NMR chemical shifts, multiplet patterns, "through-space" $^{5,6,7}J_{FF}$ values, and 2D COSY correlations contain structural information that can further narrow down the list of likely addition patterns for fullerene$(CF_3)_n$ compounds, especially when coupled with DFT-predicted relative energies and HOMO−LUMO gaps.[1,2,13,14] Finally, trifluoromethylfullerenes (TMFs) generally form crystals that allow precise X-ray structures to be determined. Given the tendency of crystalline fullerene derivatives to exhibit disorder and the tendency of CF_3 groups to exhibit librational or rotational disorder in the solid state, X-ray structures of many TMFs with surprisingly small atomic displacement parameters and without significant disorder have been determined. For example, two of the most precise X-ray structures of any fullerene or fullerene derivative are (i) an isomer of $C_{60}(CF_3)_{12}$ (cage C−C distance esd = 0.001 Å)[9] and (ii) $C_{74}(CF_3)_{12}$ (cage C−C distance esd ≤ 0.002 Å).[15]

Detailed electrochemical and DFT studies of 18 $C_{60}(CF_3)_n$ and 17 $C_{70}(CF_3)_n$ derivatives were recently published.[1,2] It was shown that the CF_3 addition pattern is as important, if not more important in many cases, as the number of CF_3 groups, n, in determining $E_{1/2}$ values. For example, isomers of $C_{60}(CF_3)_{12}$ can be either 0.32 V easier to reduce or 0.13 V harder to reduce than C_{60} itself.[1] Furthermore, two isomers of $C_{60}(CF_3)_{10}$ that differ only in the location of a single CF_3 group on the same pentagon have $C_{60}(CF_3)_{10}^{0/-}$ $E_{1/2}$ values that differ by 0.40 V.[1] It was only because a sufficiently large number of derivatives were available that correlations between $E_{1/2}$ values and addition patterns were discovered, the most important being that addition patterns with double bonds in pentagons having two C(sp^2) nearest neighbors result in the strongest electron acceptors.[1]

The trifluoromethylation of fullerenes can also lead to the discovery of previously unknown isolated-pentagon-rule (IPR)[16] hollow-higher-fullerene (HHF) cages or the verification of proposed IPR HHF cages. The reaction of a complex mixture of insoluble HHFs with CF_3I at 500 °C produced a series of HHF$(CF_3)_{12}$ compounds, six of which had their addition patterns determined by a combination of ^{19}F NMR spectroscopy and DFT calculations[17] (and two were later characterized by X-ray crystallography[15]). These six compounds are listed in Table 1 and are shown as Schlegel diagrams in Figure 1. This set of compounds provided the first experimental evidence for the existence of the HHFs C_{76}-T_d(2), C_{78}-D_{3h}(5), C_{80}-C_{2v}(5), and C_{82}-C_2(5) in arc-discharge soots and verified the D_{3h} IPR isomer of C_{74}. In a preliminary report, we published the X-ray structure of C_1-$C_{84}(CF_3)_{12}$ (one of the compounds prepared in this study), which verified the previously proposed structure of C_{84}-C_2(11).[18]

We now report a series of high-temperature reactions of soluble HHFs with CF_3I. Twenty-one new HHF$(CF_3)_n$ derivatives were isolated and characterized (n = 6−14), including nine derivatives of C_{76}-D_2(1), one derivative of C_{78}-D_3(1), two derivatives each of C_{78}-C_{2v}(2) and C_{78}-C_{2v}(3), one derivative of a C_{78} cage yet to be determined, two derivatives of C_{84}-D_2(22), one derivative of C_{84}-C_2(11), two derivatives of C_{84} cages yet to be determined, one derivative of C_{90}-C_1(32), and one derivative of a C_{90} cage yet to be determined. These are also listed in Table 1. Twelve of them with unprecedented addition patterns now known with a high degree of confidence are shown in Figure 1.

Experimental Section

Reagents and Solvents. The composite graphite rod electrodes containing ca. 1% by mass metallic cerium, lanthanum, or yttrium were prepared as previously described.[19] The following were used as received from the indicated supplier: HPLC-grade 1,2-dichlorobenzene (DCB), toluene, xylene, and heptane (Sigma-Aldrich); *N*,*N*-dimethylformamide (DMF) and hexafluorobenzene (Sigma-Aldrich); chloroform-*d* (Cambridge Isotopes); and trifluoroiodomethane (Synquest).

Arc-Discharge Synthesis and Purification of Hollow Higher Fullerenes (HHFs). Fullerene-containing soot was generated in an electric reactor by the dc arc-discharge method as previously described.[20,21] The optimal conditions of arc evaporation of the

(5) Echegoyen, L. E.; Djojo, F. D.; Hirsch, A.; Echegoyen, L. *J. Org. Chem.* **2000**, *65*, 4994–5000.
(6) Marchesan, S.; da Ros, T.; Prato, M. *J. Org. Chem.* **2005**, *70*, 4706–4713.
(7) Kareev, I. E.; Kuvychko, I. V.; Lebedkin, S. F.; Miller, S. M.; Anderson, O. P.; Seppelt, K.; Strauss, S. H.; Boltalina, O. V. *J. Am. Chem. Soc.* **2005**, *127*, 8362–8375.
(8) Kareev, I. E.; Kuvychko, I. V.; Popov, A. A.; Lebedkin, S. F.; Miller, S. M.; Anderson, O. P.; Strauss, S. H.; Boltalina, O. V. *Angew. Chem., Int. Ed.* **2005**, *44*, 7984–7987.
(9) Troyanov, S. I.; Dimitrov, A.; Kemnitz, E. *Angew. Chem., Int. Ed.* **2006**, *45*, 1971–1974.
(10) Kareev, I. E.; Shustova, N. B.; Kuvychko, I. V.; Lebedkin, S. F.; Miller, S. M.; Anderson, O. P.; Popov, A. A.; Strauss, S. H.; Boltalina, O. V. *J. Am. Chem. Soc.* **2006**, *128*, 12268–12280.
(11) Omelyanyuk, N. A.; Goryunkov, A. A.; Tamm, N. B.; Avdoshenko, S. M.; Ioffe, I. N.; Sidorov, L. N.; Kemnitz, E.; Troyanov, S. I. *Chem. Commun.* **2007**, 4794–4796.
(12) Fowler, P. W.; Redmond, D. B.; Sandall, J. P. B. *J. Chem. Soc., Faraday Trans.* **1998**, *94*, 2883–2887.
(13) Dorozhkin, E. I.; Ignat'eva, D. V.; Tamm, N. B.; Goryunkov, A. A.; Khavrel, P. A.; Ioffe, I. N.; Popov, A. A.; Kuvychko, I. V.; Streletskiy, A. V.; Markov, V. Y.; Spandl, J.; Strauss, S. H.; Boltalina, O. V. *Chem. Eur. J.* **2006**, *12*, 3876–3889.
(14) Kareev, I. E.; Shustova, N. B.; Peryshkov, D. V.; Lebedkin, S. F.; Miller, S. M.; Anderson, O. P.; Popov, A. A.; Boltalina, O. V.; Strauss, S. H. *Chem. Commun.* **2007**, 1650–1652.
(15) Shustova, N. B.; Popov, A. A.; Newell, B. S.; Miller, S. M.; Anderson, O. P.; Seppelt, K.; Bolskar, R. D.; Boltalina, O. V.; Strauss, S. H. *Angew. Chem., Int. Ed.* **2007**, *46*, 4111–4114.
(16) Fowler, P. W.; Manolopoulous, D. E. *An Atlas of Fullerenes*; Dover: Mineola, NY, 2006.
(17) Shustova, N. B.; Kuvychko, I. V.; Bolskar, R. D.; Seppelt, K.; Strauss, S. H.; Popov, A. A.; Boltalina, O. V. *J. Am. Chem. Soc.* **2006**, *128*, 15793–15798.
(18) Kareev, I. E.; Kuvychko, I. V.; Shustova, N. B.; Lebedkin, S. F.; Bubnov, V. P.; Anderson, O. P.; Popov, A. A.; Strauss, S. H.; Boltalina, O. V. *Angew. Chem., Int. Ed.* **2008**, *47*, 6204–6207.
(19) Kareev, I. E.; Bubnov, V. P.; Yagubskii, E. B. *Russ. Chem. Bull., Int. Ed.* **2007**, *56*, 2140–2144.
(20) Bubnov, V. P.; Krainskii, I. S.; Laukhina, E. E.; Yagubskii, E. B. *Russ. Chem. Bull.* **1994**, *5*, 746–750.

Table 1. Isolated and Characterized Trifluoromethylated Hollow Higher Fullerenes[a]

compd	overall symmetry	addition pattern	cage isomer	IUPAC lowest locants for known/proposed structures	CF_3 groups on ICCB C atoms	HOMO−LUMO gap (DFT), eV
74-12-1[b,c]	C_2	p^{11}	$D_{3h}(1)$	2,5,11,19,27,37,43,47,52,56,62,68	none	2.17
76-6-1	C_1	p^5	$D_2(1)$	5,20,44,47,68,71	none	1.56
76-8-1	C_1	p^5,p	$D_2(1)$	5,20,38,44,47,59,68,71	C38, C59	1.54
76-8-2	C_1	p^5,p	$D_2(1)$	5,12,20,31,44,47,68,71	none	1.82
76-10-1	C_2	p^4,p^4	$D_2(1)$	5,12,20,31,44,47,55,58,61,68	none	2.00
76-10-2	C_1	p^5,p,p	$D_2(1)$	5,12,20,31,38,44,47,59,68,71	none	1.60
76-10-3	C_1	p^5,p,p	$D_2(1)$	5,12,20,31,37,44,47,60,68,71	C37, C60	1.58
76-10-4	C_1	$4+3+3$	$D_2(1)$		not known	
76-10-5	C_1	p^5,p,p	$D_2(1)$	5,12,20,31,36,39,44,47,68,71	C36, C39	1.57
76-12-1[b]	C_s	p^9-loop,p^2	$T_d(2)$	7,14,17,23,32,37,46,51,60,68,71,74	none	2.06
76-12-2	C_2	p^3mp,p^3mp	$D_2(1)$	6,9,15,30,33,35,42,44,47,62,68,71	C8, C24, C53, C69	1.67
78-8-1	C_2	p^7	$C_{2v}(3)$	2,5,11,19,31,42,45,55	none	1.91
78-10-1	C_2	p^4,p^4	$D_3(1)$	11,16,26,30,36,41,49,55,58,68	none	1.94
78-10-2	C_s	p^9	$C_{2v}(2)$	25,34,37,46,50,55,60,65,69,72	none	1.57
78-10-3[e]	C_2	p^4,p^4	$C_{2v}(2)$	25,34,37,46,50,55,60,65,69,74	none	1.36
78-12-1[b,c]	C_2	p^{11}	$D_{3h}(5)$	7,14,19,23,32,39,46,51,58,66,69,74	none	2.09
78-12-2	C_1	p^5mp,p^3	$C_{2v}(3)$	2,5,11,19,27,30,35,42,45,58,70,73	C27, C30	1.86
78-14-1	C_1	$11+3$	−[d]		not known	
80-12-1[b]	C_s	p^{10}-loop,p	$C_{2v}(5)$	3,6,35,39,43,46,50,54,58,62,67,71	none	1.93
82-12-1[b]	C_2	p^{11}	$C_2(5)$	3,6,9,17,26,37,50,53,61,64,67,74	none	1.80
82-12-2[b]	C_2	p^5,p^5	$C_2(3)$	7,15,24,31,35,42,45,52,56,63,71,78	none	2.08
84-10-1	C_1	$x+y=10$	−[d]		not known	
84-12-1	D_2	p^5,p^5	$D_2(22)$	3,6,9,17,29,39,44,54,66,74,81,84	none	2.08
84-12-2[f]	C_1	p^6,p^2,p	$C_2(11)$	7,18,21,29,35,50,55,59,67,78,83,84	none	1.56
84-12-3	C_2	p^5,p^5	$D_2(22)$	2,5,11,19,27,37,44,54,66,74,81,84	none	1.55
84-14-1	C_1	$x+y=14$	−[d]		not known	
90-12-1	C_1	$(x+y=8)+2+2$	−[d]		not known	
90-12-2	C_1	p^7,p,p	$C_1(32)$	23,26,30,34,45,50,54,58,62,65,69,85	none	1.36

[a] All compounds from this work unless otherwise indicated. All compounds have been characterized by ^{19}F NMR spectroscopy. The following compounds have also been characterized by single-crystal X-ray diffraction: **74-12-1** (ref 15), **78-10-1** (this work), **78-10-2** (this work), **78-12-1** (ref 15), **78-12-2** (this work), and **84-12-2** (ref 18). IUPAC-numbered Schlegel diagrams and a list of cage rings or C atoms through which symmetry axes pass are available in the Supporting Information. ICCB = interpentagonal C−C bond. [b] Reference 17. [c] Reference 15. [d] The particular cage isomer is unknown at this time. [e] This is a tentative cage and addition-pattern assignment because of the somewhat low DFT-predicted HOMO−LUMO gap. [f] Reference 18.

metal-doped graphite rod electrodes were as follows: He pressure, 120 Torr; dc current, 80−90 A; voltage, 28−30 V; arc length, 5 mm; distance between arc and cooled reactor wall, 50 mm; evaporation rate, 5 mm min^{-1}. Fullerenes were extracted from the soots in two stages. The first involved extractions into five portions of DCB; the second involved extractions into seven portions of DMF. The DMF extracts contained endohedral metallofullerenes and were not used in this work. The DCB extracts were evaporated to dryness, redissolved in xylene, and purified by HPLC using a 20 mm i.d. × 250 mm Cosmosil Buckyprep column (Nacalai Tesque, Inc.): 16 mL min^{-1} toluene eluent; 330 nm UV detection). The fraction that eluted between 0 and 18 min contained C_{60} and C_{70} and was not used further in this work. The fraction that eluted between 18 and 27 min contained C_{76} and C_{78} isomers. A third fraction was obtained by changing the eluent to DCB; this fraction contained fullerenes larger than C_{78}. Additional processing of the 18−27 min toluene fraction resulted in the isolation of 98+% pure C_{76} and a mixture of isomers of C_{78}, as shown in Figure 2. Each of these samples was 5–7 mg. A larger sample of the DCB extract was processed to remove C_{60} and C_{70} and contained HHFs from C_{76} to C_{90}. This HHF sample was ca. 80 mg.

Preparation of HHF$(CF_3)_n$ Derivatives. The high-temperature trifluoromethylations of the three HHF samples were carried out as previously described.[7] The 5–7 mg samples of C_{76}-$D_2(1)$ and isomers of C_{78} were first heated to 520 °C under an Ar atmosphere, after which an atmosphere of CF_3I was passed through the hot tube for 1 h. The 80 mg sample of HHFs was first heated to 520 °C under Ar, after which CF_3I was passed through the hot tube for 2 h as the temperature was slowly raised from 520 to 550 °C. In all three reactions, virtually all of the fullerenes were converted to volatile orange and brown products, which, along with purple I_2, condensed in the cold part of the reaction tube outside the furnace. Iodine was removed by heating the condensed crude products to 150 °C in a stream of argon. The HHF$(CF_3)_n$ products were dissolved in toluene and processed by HPLC as above except that either toluene, heptane, or mixtures of toluene and heptane were used as eluents. Retention times are listed in Table S-2 (Supporting Information). The purified compounds were characterized by negative-ion atmospheric-pressure chemical-ionization mass spectrometry (NI-APCI-MS) and by ^{19}F NMR spectroscopy.

Physicochemical Measurements. Matrix-assisted laser desorption−ionization (MALDI) time-of-flight mass spectra were recorded using a Voyager-DE PRO workstation (Applied Biosystems). Sulfur was used as the matrix material. It was mixed with the sample in toluene or toluene−hexane immediately prior to deposition on the target. Nitrogen laser pulses of 337 nm wavelength, 0.5 ns duration, and 3 Hz frequency were used to desorb the species into the gas phase. The negative or positive ions formed were detected in reflectron mode. APCI mass spectra were recorded using a ThermoQuest Finnegan LCQ-DUO spectrometer. Fluorine-19 NMR spectra were recorded using a Bruker INOVA-400 spectrometer (376.5 MHz, 25 °C, chloroform-*d*, C_6F_6 internal standard (δ −164.9)).

X-ray Diffraction. Experimental details of the three structure determinations are listed in Table 2. Crystals of **78-10-1** were grown from a mixture of toluene, dichlorobenzene, and heptane. X-ray diffraction data were obtained by using a Bruker Kappa APEX II CCD diffractometer (Mo Kα radiation ($\lambda = 0.71073$ Å), graphite monochromator). Absorption and other corrections were applied by using SADABS.[22] The structure was solved by using direct methods and refined (on F^2, using all data) by a full-matrix,

(21) Bubnov, V. P.; Laukhina, E. E.; Kareev, I. E.; Koltover, V. K.; Prokhorova, T. G.; Yagubskii, E. B.; Kozmin, Y. P. *Chem. Mater.* **2002**, *14*, 1004–1008.

(22) Sheldrick, G. M. *SADABS*: A program for area detector absorption corrections. Bruker AXS Inc.: Madison, 2003.

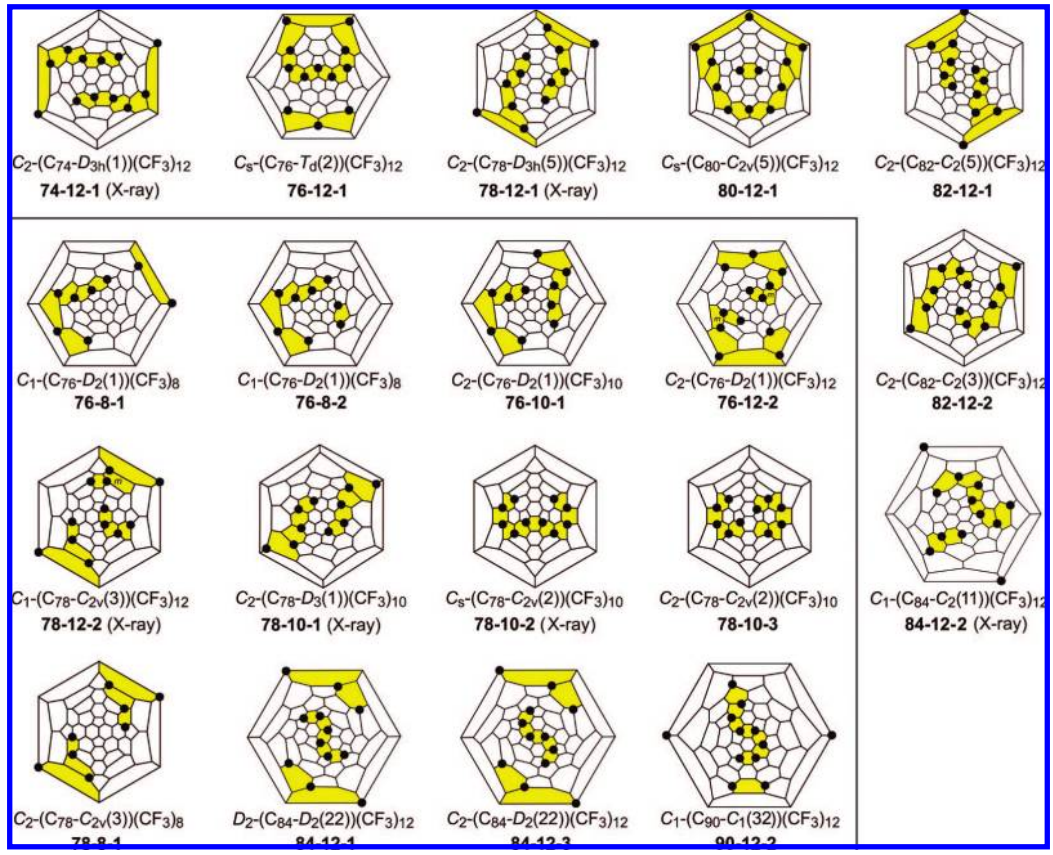

Figure 1. Schlegel diagrams of CF_3 derivatives of hollow higher fullerenes (HHFs) that have been structurally characterized by ^{19}F NMR spectroscopy, by DFT calculations, and in six cases by single-crystal X-ray diffraction. The compounds above and to the right of the line were reported in refs15, 17, and 18. The compounds below and to the left of the line are reported in this work. The Schlegel diagram for **76-6-1** is the same as the one for **76-8-1** or **76-8-2** minus the two CF_3 groups the isolated *p*-$C_6(CF_3)_2$ hexagon.

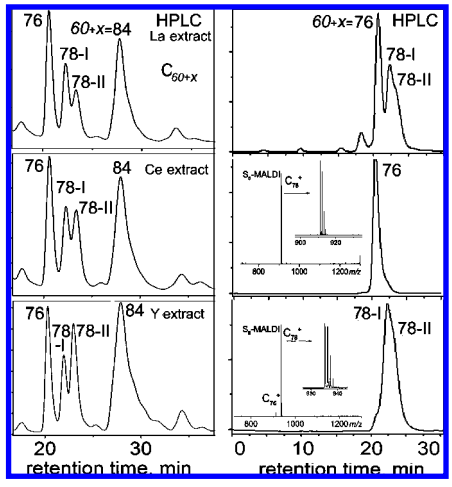

Figure 2. Left column: HPLC traces showing the HHF fractions of the extracts obtained from arc-discharge soots prepared using graphite rod electrodes doped with lanthanum, cerium, or yttrium. Right column: HPLC traces showing the process of purification of C_{76} and of isomers of C_{78}. Insets: S_8-MALDI mass spectra of the purified C_{76} and C_{78} samples.

Table 2. Crystal Data and Structure Refinement Parameters for **78-10-1**, **78-10-2**, and **78-12-2**[a]

	78-10-1	**78-10-2** · C_7H_8	**78-12-2** · C_6H_5Br
molecular formula	$C_{88}F_{30}$	$C_{95}H_8F_{30}$	$C_{96}H_5BrF_{36}$
formula weight, g mol^{-1}	1626.88	1719.01	1921.91
crystal system	monoclinic	monoclinic	monoclinic
space group	*C*2/*c*	$P2_1/m$	$P2_1/c$
Z	4	2	4
color of crystal	red	red	yellow
unit cell dimensions			
a, Å	23.8603(7)	11.442(2)	18.526(5)
b, Å	11.1601(4)	18.791(4)	14.922(5)
c, Å	22.9338(7)	14.883(3)	26.019(8)
α, deg	90	90	90
β, deg	105.447(2)	110.05(1)	96.030(8)
γ, deg	90	90	90
temperature, K	100(1)	100(1)	173(2)
final *R* indices[b] [$I > 2\sigma(I)$]			
R_1	0.044	0.056	0.067
wR_2	0.120	0.15	0.166
goodness-of-fit on F^2	1.051	1.071	1.072

[a] **78-10-1** = 11,16,26,30,36,41,49,55,58,68-(C_{78}-D_3(1))$(CF_3)_{10}$; **78-10-2** = 25,34,37,46,50,-55,60,65,69,72-(C_{78}-C_{2v}(2))$(CF_3)_{10}$; **78-12-2** = 2,5,11,19,27,30,35,42,45,58,70,73(C_{78}-C_{2v}(3))-$(CF_3)_{12}$. [b] $R_1 = (\sum||F_o| - |F_c||)/\sum|F_o|$; $wR_2 = (\sum[w(F_o^2 - F_c^2)^2]/\sum[w(F_o^2)^2])^{1/2}$.

weighted least-squares process using Bruker SHELXL software.[23,24] Standard refinement led to chemically unreasonable electron density in parts of the solvent-occupied regions of the structure. The best residual indices were obtained from a model for which the program SQUEEZE[25] was used to fill the disordered solvent regions; we report this model for **78-10-1** here.

Crystals of **78-10-2**·C_8H_7 were grown from a mixture of toluene and heptane. X-ray diffraction data were also obtained by using a Bruker Kappa APEX II CCD diffractometer (Mo Kα radiation (λ = 0.71073 Å), graphite monochromator). Absorption and other corrections were applied by using SADABS.[22] The structure was solved by using direct methods and refined (on F^2, using all data) by a full-matrix, weighted least-squares process. Non-hydrogen atoms were refined by using anisotropic displacement parameters. Hydrogen atoms were placed in idealized positions and refined by

using a riding model. Bruker APEX2 software was employed for data collection and reduction, and Bruker SHELXTL[23,24] software was used for structure solution, refinement, and graphics.

Crystals of **78-12-2** were grown from a saturated bromobenzene solution that contained some *p*-xylene from earlier crystallization attempts. X-ray diffraction data were recorded on a Bruker Smart CCD 1000 diffractometer employing Mo Kα radiation (graphite monochromator), a scan width of 0.3° in ω, and a measuring time of 40 s frame^{-1}, obtaining a full shell of 1800 frames up to $2\theta = 46.0°$. The structure was solved by using direct methods and refined (on F^2, using all data) by a full-matrix, weighted least-squares process. An absorption correction was applied by equalizing symmetry-related reflections using the program SADABS,[22] as implemented in the Bruker software. One bromobenzene molecule was easily identified; a second solvent molecule (without heavy atoms, therefore probably *p*-xylene) was severely disordered. Since no disorder model was successful, the program SQUEEZE[25] was used to generate a data set that ignores the contribution of this (and only this) disordered solvent. All non-hydrogen atoms were refined by using anisotropic displacement parameters. Hydrogen atoms were placed in idealized positions and refined by using a riding model. Bruker software was employed for data collection and reduction, and Bruker SHELXTL software was used for structure solution, refinement, and graphics.[23]

Results and Discussion

I. Synthesis and HPLC Purification of Soluble Hollow Higher Fullerenes (HHFs). The number of molecular carbon allotropes known as fullerenes continues to grow each year. Nine have been unambiguously proven to exist by single-crystal X-ray diffraction studies of the bare cages or their derivatives (not counting endohedral fullerenes, since their existence alone does not prove the existence of the corresponding hollow cage): C_{60};[26,27] C_{70};[27,28] C_{74}-$D_{3h}(1)$;[15] C_{76}-$D_2(1)$;[29] C_{78}-$C_{2v}(2)$ and C_{78}-$C_{2v}(3)$;[30] C_{78}-$D_{3h}(5)$;[15] C_{84}-$C_2(11)$;[18] and C_{84}-$D_{2d}(23)$.[31] More than a dozen more have been identified using NMR spectra of the bare cages[32,33] or derivatives,[17] including seven additional IPR isomers of C_{84}.[34,35] The existence of three IPR fullerene cages has been verified during the course of this work, two by X-ray diffraction, C_{78}-$D_3(1)$ and C_{84}-$C_2(11)$, and one by NMR spectroscopy, C_{90}-$C_1(32)$ (the X-ray structure of C_1-(C_{84}-$C_2(11)$)$(CF_3)_{12}$ was briefly reported in a recent communication[18]).

The study of HHFs is hampered by the limited access to relatively pure cage isomers. They are generally present in small amounts in carbon arc-discharge soots and are very expensive.[36] In unpublished work, some of us (I.E.K. and V.P.B.) have demonstrated that doping graphite rod electrodes with rare earth metals can increase the amount of HHFs in the soots by a factor of 2−3. A related finding was reported by Dennis et al. in 1998.[37] They found that doping graphite rods with gadolinium enhanced the production of some isomers of C_{84} at the expense of other C_{84} isomers. In order to increase the amounts of HHFs available for our trifluoromethylation studies, we generated arc-discharge soots using graphite electrodes doped with the rare-earth metals lanthanium, cerium, or yttrium.

The left column in Figure 2 shows HPLC traces of the extracts prepared with the metal-doped graphite rods. Note that the relative amount of C_{76} is higher in the "La extract" than in the others and that the relative amounts of the two C_{78} fractions are highly dependent on which metal was doped into the graphite electrodes. A more extensive quantitative analysis of these and other results will be published separately. For the purposes of preparing HHF$(CF_3)_n$ products in this work, the more abundant "La extract" was further processed by HPLC, as shown in the right column in Figure 2. Note that the sample of C_{76} that was collected was very pure, whereas the mixture of C_{78} isomers contained a small amount of C_{76}. The mixture of C_{78} isomers contained not only the two known "major" isomers, C_{78}-$C_{2v}(2)$ and C_{78}-$C_{2v}(3)$,[38,39] but a significant amount of the C_{78}-$D_3(1)$ cage, as evidenced by the isolation and structural characterization of C_2-(C_{78}-$D_3(1)$)$(CF_3)_{10}$ (**78-10-1**, see below).

II. Synthesis and HPLC Purification of HHF$(CF_3)_n$ Compounds. A. General Comments. The 21 new compounds are listed in Table 1, along with seven previously reported HHF$(CF_3)_{12}$ derivatives. Assignments of overall symmetry, addition pattern, fullerene cage isomer, and IUPAC lowest locants[40] will be discussed in appropriate sections below. Schlegel diagrams for **78-12-2** and 11 of the new compounds with confirmed or "most-likely" proposed addition patterns are shown in Figure 1 (the compound **78-12-2** was reported previously,[17] but its structure was not established until now).

The HHF$(CF_3)_n$ compounds were prepared by treating solid samples containing one or more soluble HHFs with a continuous flow of gaseous CF_3I (1 atm) in a hot tube at 520−550 °C, as shown in eq 1 ($n = 6, 8, 10, 12, 14$).

$$\text{HHF(s)} + \text{excess } CF_3I(g) \xrightarrow{520-550\ ^\circ C} \xrightarrow[\text{condensation}]{\text{cold zone}} \text{HHF}(CF_3)_n(s) + (n/2)I_2(s) \quad (1)$$

As discussed in our previous work with C_{60}, C_{70}, and insoluble HHFs,[1,2,7,17] the range of n values for fullerene$(CF_3)_n$ reaction products depends on temperature, the length and diameter of the hot tube, and the CF_3I flow rate. In this work, the conditions were adjusted so that relatively narrow ranges of HHF$(CF_3)_n$ compounds were prepared, and the most abundant compounds in the product mixtures that were purified and characterized had

(23) Sheldrick, G. M. *Acta Crystallogr., Sect. A* **2008**, *64*, 112–122.
(24) Sheldrick, G. M. *SHELXTL*, v. 6.14; Bruker AXS: Madison, WI, 2004.
(25) van der Sluis, P.; Spek, T. *Acta Crystallogr., Sect. A* **1990**, *46*, 194–201.
(26) Olmstead, M. M.; de Bettencourt-Dias, A.; Lee, H. M.; Pham, D.; Balch, A. L. *Dalton Trans.* **2003**, 3227–3232.
(27) Neretin, I. S.; Slovokhotov, Y. L. *Russ. Chem. Rev.* **2004**, *73*, 455–486.
(28) Pham, D.; Ceron-Bertran, J.; Olmstead, M. M.; Mascal, M.; Balch, A. L. *Cryst. Growth Design* **2007**, *7*, 75–82.
(29) Simeonov, K. S.; Amsharov, K. Y.; Jansen, M. *Angew. Chem., Int. Ed.* **2007**, *46*, 841–8421.
(30) Troyanov, S. I.; Kemnitz, E. *Eur. J. Org. Chem.* **2003**, 3916–3919.
(31) Balch, A. L.; Ginwalla, A. S.; Lee, J. W.; Noll, B. C.; Olmstead, M. M. *J. Am. Chem. Soc.* **1994**, *116*, 2227–2228.
(32) Thilgen, C.; Diederich, F. *Chem. Rev.* **2006**, *106*, 5049–5135.
(33) Hirsch, A.; Brettreich, M. *Fullerenes—Chemistry and Reactions*; Wiley-VCH: Weinheim, 2005.
(34) Dennis, T. J. S.; Kai, T.; Tomiyama, T.; Shinohara, H. *Chem. Commun.* **1998**, 619–620.
(35) Dennis, T. J. S.; Kai, T.; Asato, K.; Tomiyama, T.; Shinohara, H.; Yoshida, T.; Kobayashi, Y.; Ishiwatari, H.; Miyake, Y.; Kikuchi, K.; Achiba, Y. *J. Phys. Chem. A* **1999**, *103*, 8747–8752.
(36) Five milligrams of 98% pure C_{84} (a mixture of isomers) is currently priced at $799 (http://www.sigmaaldrich.com/catalog/search/ProductDetail/ALDRICH/482986/, April 2008).
(37) Tagmatarchis, N.; Avent, A. G.; Prassides, K.; Dennis, T. J. S.; Shinohara, H. *Chem. Commun.* **1999**, 1023–1024.
(38) Diederich, F.; Whetten, R. L.; Thilgen, C.; Ettl, R.; Chao, I.; Alvarez, M. M. *Science* **1991**, *254*, 1768–1770.
(39) Kikuchi, K.; Nakahara, N.; Wakabayashi, T.; Suzuki, S.; Shiromaru, H.; Miyake, Y.; Saito, K.; Ikemoto, I.; Kainosho, M.; Achiba, Y. *Nature* **1992**, *357*, 142–145.
(40) Cozzi, F.; Powell, W. H.; Thilgen, C. *Pure Appl. Chem.* **2005**, *77*, 843–923.

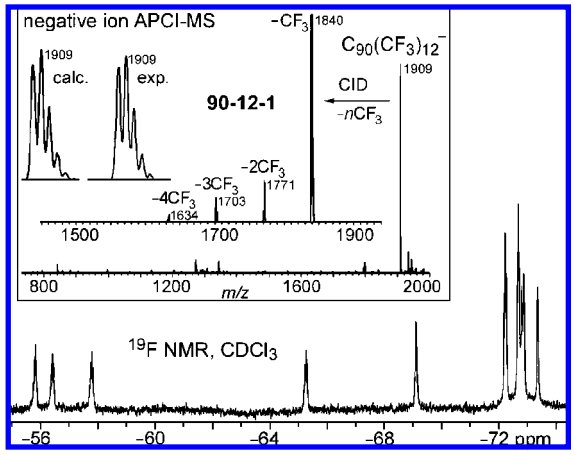

Figure 3. Fluorine-19 NMR spectrum of **90-12-1** (376.5 MHz, C_6F_6 internal standard (δ −164.9)). Inset: Negative-ion APCI mass spectrum of **90-12-1**, CID mass spectrum of the *m/z* 1909 peak showing consecutive loss of CF_3 groups, and calculated and experimental mass spectra of $C_{90}(CF_3)_{12}$ isotopomers.

either 10 or 12 CF_3 substituents (note that the IUPAC has recommended that the term "substituent" be used instead of the term "addend" for the purpose of nomenclature[41]). These compositions were of particular interest because their addition patterns could be analyzed using structural principles first formulated for $HHF(CF_3)_{12}$ compounds in our previous paper.[17] Another reason for targeting these compositions is that fullerene$(CF_3)_n$ compounds with $n > 12$ have short HPLC retention times (even using nonpolar eluents such as heptane) and therefore are more difficult to separate using semi-preparative or preparative HPLC columns.

The compositions and isomeric purities of the $HHF(CF_3)_n$ compounds were determined by NI-APCI-MS and ^{19}F NMR spectroscopy, respectively. For example, the ^{19}F NMR spectrum and NI-APCI and CID mass spectra of **90-12-1** are shown in Figure 3. It can be seen that the compound does have the composition $C_{90}(CF_3)_{12}$ and is 95+% pure.

Although the trifluoromethylation reactions were performed at temperatures above 500 °C, fullerenes are not known to undergo cage isomerization, even at higher temperatures. Therefore, each of the $C_{76}(CF_3)_n$ compounds we isolated must be a derivative of C_{76}-D_2(1), and each of the $C_{78}(CF_3)_n$ compounds must be a derivative of C_{78}-D_3(1), C_{78}-C_{2v}(2), or C_{78}-C_{2v}(3).

B. Trifluoromethylation of C_{76}. The reaction of C_{76}-D_2(1) with CF_3I at 520 °C yielded a mixture of products in which $C_{76}(CF_3)_{10}$ was the dominant composition and **76-10-1** was the dominant isomer. The left column in Figure 4 shows the stages of the HPLC purification procedure for the $C_{76}(CF_3)_n$ products. The products were first separated into two fractions using toluene as the eluent. Fraction 1 was reprocessed using 30/70 v/v toluene/heptane as the eluent, resulting in a single dominant fraction labeled fraction 1-2. According to NI-APCI-MS and NMR spectra, this was the single isomer **76-10-1**. Four other isomers of $C_{76}(CF_3)_{10}$ were isolated from fraction 2. Fraction 1-1 contained other $C_{76}(CF_3)_n$ compounds, of which one, **76-12-2**, was purified and characterized.

There is a striking similarity of the product ratios for the $C_{76}(CF_3)_n$ compounds and for isomers of $C_{70}(CF_3)_n$[2] for a given

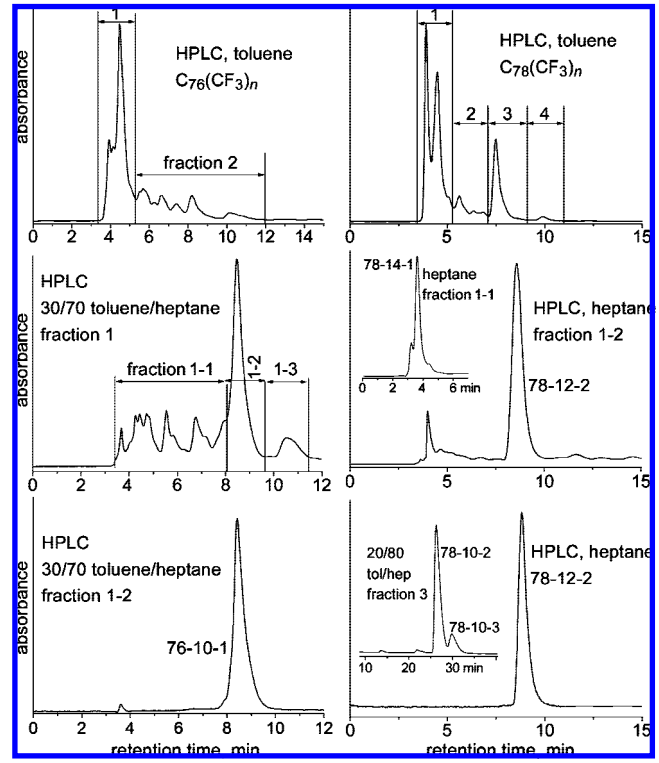

Figure 4. Left column: HPLC traces showing the stages of purification of **76-10-1** from the crude reaction product. Right column: HPLC traces showing the stages of purification of **78-14-1**, **78-12-2**, **78-10-2**, and **78-10-3**. A 20 mm i.d. × 250 mm Cosmosil Buckyprep HPLC column was used for these purifications (16 mL min^{-1} flow rate; 330 nm detection).

value of *n*. For example, both fullerenes form a single isomer with $n = 10$ in much greater abudance than other $C_{70,76}(CF_3)_{10}$ isomers (there are a total of five isomers of $C_{76}(CF_3)_{10}$ and seven isomers of $C_{70}(CF_3)_{10}$[2]). The regioselectivity of multiple CF_3 radical additions appears to be higher for C_{70} and C_{76} than for C_{60}, which forms seven isomers of $C_{60}(CF_3)_{10}$ of comparable abundance.[1]

C. Trifluoromethylation of C_{78}. The HPLC trace of the crude mixture of $C_{78}(CF_3)_n$ products is different than that of the $C_{76}(CF_3)_n$ in that there were three fractions of comparable abundance. The right column in Figure 4 shows the stages of the HPLC purification procedure for the $C_{78}(CF_3)_n$ products. A total of four fractions were collected, and each contained a single dominant compound, **78-14-1**, **78-12-2**, **78-10-2**, and **78-8-1** (the fourth fraction, albeit a minor amount of the mixture of products, was the pure single-isomer derivative **78-8-1**). Fraction 1, in addition to **78-14-1**, contained the minor isomer **78-10-1**, and fraction 3, in addition to **78-10-2**, contained the minor isomer **78-10-3** (ca. 10−15% relative to **78-10-2**, assuming that both compounds have equal extinction coefficients at 330 nm). See Table S-2 for HPLC retention times. The HPLC traces in the right column of Figure 4 demonstrate that HPLC retention times generally decrease as the number of CF_3 substitutents increases.

D. Trifluoromethylation of a Mixture of HHFs. An 80 mg sample of a mixture of soluble HHFs from which C_{60} and C_{70} had been removed was reacted with CF_3I at 520−550 °C. The HPLC and MS data obtained for the $HHF(CF_3)_n$ mixture of products revealed the presence of some of the $C_{78}(CF_3)_n$ compounds that were abundant when the purified sample of C_{78} isomers was used: **78-12-2** and **78-10-2**. In addition, $C_{82}(CF_3)_n$ and $C_{84}(CF_3)_n$ derivatives were also abundant in the mixture,

(41) Powell, W. H.; Cozzi, F.; Moss, G. P.; Thilgen, C.; Hwu, R. J. R.; Yerin, A. *Pure Appl. Chem.* **2002**, *74*, 629–695.

in accordance with the relative abundances of these HHFs in the DCB extract. In previous work, we demonstrated that higher trifluoromethylation temperatures result in lower values of n for $C_{60,70}(CF_3)_n$ compounds.[1,2,7] Since the temperature of the reaction of CF_3I with the mixture of HHFs was slightly higher than for the reactions of CF_3I with purified samples of C_{76}-D_2(1) and C_{78} isomers, it is not surprising that the overall composition shifted slightly toward lower values of n. For example, we were able to isolate and characterize an isomer of $C_{76}(CF_3)_6$ (**76-6-1**), two isomers of $C_{76}(CF_3)_8$ (**76-8-1** and **-2**), and a significant amount of an isomer of $C_{78}(CF_3)_8$ (**78-8-1**). Therefore, the temperature-dependence trend observed earlier in the synthesis of $C_{60,70}(CF_3)_n$ derivatives is also followed in syntheses of $HHF(CF_3)_n$ derivatives.

Our results for the mixture of HHFs show that the ranges of n values included lower values of n for smaller HHFs, such as C_{76}-D_2(1) and isomers of C_{78}, than for larger HHFs including isomers of C_{82}, C_{84}, and C_{90}. For example, the observed ranges for C_{76}, C_{78}, and C_{84} were $n = 6-10$, $8-12$, and $10-14$, respectively. This is probably because $HHF(CF_3)_n$ compounds for a given value of n are more volatile for smaller HHFs than for larger HHFs, and thus they sublime out of the hot zone before more CF_3 groups are added to the cage. Therefore, it should be possible in the future (when larger amounts of HHFs become available) to optimize reaction conditions to obtain higher yields of $HHF(CF_3)_n$ products with particular compositions.

Finally, for a given set of HPLC conditions and fewer than 12 CF_3 groups, a larger carbon-cage derivative appears to have a longer retention time, in general, than a smaller carbon-cage derivative. For example, the following order of retentions times was observed: $C_{60}(CF_3)_{10}$ isomers < $C_{70}(CF_3)_{10}$ isomers < $C_{76}(CF_3)_{10}$ isomers < $C_{78}(CF_3)_{10}$ isomers < $C_{84}(CF_3)_{10}$ (**84-10-1**) (see also Table S-2). The remarkable sensitivity of the Buckyprep HPLC column, not only for HHF separations, for which the column was designed, but also for the $HHF(CF_3)_n$ separations when $n \geq 6$, has allowed us to isolate and characterize 21 new $HHF(CF_3)_n$ compounds in this work, the structures/addition patterns of which will now be described.

III. Cage Isomers and Addition Patterns of $HHF(CF_3)_n$ Compounds ($6 \leq n \leq 14$). A. Background. The structure of a fullerene$(X)_n$ derivative (i.e., the particular fullerene cage isomer and the addition pattern of the substituents) determines many if not most of its physicochemical properties, from solubility to photophysical/photochemical behavior to redox potentials (or their gas-phase counterparts, electron affinities and ionization potentials) to the tendency to undergo regioselective substitution reactions or further additions.[32,33,42−45] As an example, the link between addition patterns and redox potentials for $C_{60}(CF_3)_n$ and $C_{70}(CF_3)_n$ derivatives was presented in two recent papers (and a specific link between double-bonds-in-pentagons (DBIPs) and electrochemical potentials was established).[1,2] An example of cycloaddition regioselectivity using an isomer of $C_{70}(CF_3)_{10}$ as the starting material was recently published.[46] In view of the importance of knowing the addition patterns of exohedral fullerene derivatives in order to understand and take advantage of their properties, a considerable effort was made to establish the structures of the 21 $HHF(CF_3)_n$ compounds reported in this work (their spectroscopic properties and chemical reactivities will be correlated with their addition patterns in future work). This effort will be described in the remainder of this paper.

Let us focus initially on substituents X that add to fullerenes in such a way that each forms a single bond to one fullerene C atom and that no cage C−C bonds are broken (e.g., X = H, F, Cl, Br, R, Ar, R_f, CN, etc.). In those cases, n is an even number. The steric and, to some extent, the electronic properties of the substituents determine whether or not they can be attached to the same pentagon or hexagon, including whether or not they can be attached to contiguous cage C atoms. In general, large substituents do not form structures with strings of contiguous cage C(sp^3) atoms, structures that are the rule when the substituents are small[44,47] or when the addend precursor undergoes a 1,2-cycloaddition to the cage.[32,33] For example, the DFT-predicted relative energies of *ortho*-$C_{60}F_2$ (i.e., 1,9-$C_{60}F_2$) and *para*-$C_{60}F_2$ (i.e., 1,7-$C_{60}F_2$) are 0.0 and 29.7 kJ mol^{-1}, respectively,[44] but the DFT relative energies of 1,9-$C_{60}(CF_3)_2$ and 1,7-$C_{60}(CF_3)_2$ are 34.7 and 0.0 kJ mol^{-1}, respectively[48] (IUPAC-numbered Schlegel diagrams for C_{60}[41] and other relevant fullerenes[40,41] are shown in Figures S-1−S-8 in the Supporting Information). The one exception to this rule, for large substituents, appears to be the particularly stable skew pentagonal pyramid (SPP) addition pattern of $C_{60}Br_6$,[49] $C_{60}(CF_3)_6$,[10] and one of the isomers of $C_{60}(CF_3)_{12}$ (the one with two SPP fragments),[11] among other $C_{60}(X)_6$ derivatives.[50] This exception aside, there is a tendency for 4−12 large substituents such as CF_3[1,2,15] groups or Br atoms[51] to form a ribbon of edge-sharing *meta*- and/or *para*-C_6X_2 hexagons on C_{60} or C_{70}, where each shared edge is a C(sp^3)−C(sp^2) bond. Clare and Kepert analyzed their AM1-predicted energies for $C_{60}Br_4$ and $C_{60}Br_8$ isomers and discovered that addition patterns with ribbons of C_6Br_2 hexagons were inherently more stable than addition patterns with isolated *p*-C_6Br_2 hexagons.[51] The reason for this phenomenon was not explained at the time, but in a later paper on $C_{70}(X)_n$ derivatives they stated, "The [*para*-]C_6Br_2 rings are in the boat conformation, and the end C_6Br rings which are in a half boat conformation are *predisposed* to add bromine to extend the [ribbon]" (emphasis added).[47] However, the underlying steric and/or electronic reasons *why* a half-boat conformation on the surface of a fullerene should be predisposed to become a *p*-C_6X_2 hexagon were not identified.

With significantly larger substitutents, ribbons are apparently not as stable as multiple isolated *p*-$C_6(X)_2$ hexagons, as in the structure of C_3-C_{60}(2-C_3F_7)$_6$, which has three isolated *p*-C_6(2-

(42) Guldi, D. M.; Kamat, P. V. In *Fullerenes: Chemistry, Physics, and Technology*; Kadish, K. M., Ruoff, R. S., Eds.; Wiley-Interscience: New York, 2000; pp 225−281.
(43) Xiao, Z.; Wang, F. D.; Huang, S. H.; Gan, L. B.; Zhou, J.; Yuan, G.; Lu, M. J.; Pan, J. Q. *J. Org. Chem.* **2005**, *70*, 2060–2066.
(44) Clare, B. W.; Kepert, D. L. *J. Mol. Struct. (Theochem)* **2003**, *621*, 211–231.
(45) Boltalina, O. V.; Street, J. M.; Taylor, R. *Chem. Commun.* **1998**, 1827–1828.
(46) Ovchinnikova, N. S.; Ignat'eva, D. V.; Tamm, N. B.; Avdoshenko, S. M.; Goryunkov, A. A.; Ioffe, I. N.; Markov, V. Y.; Troyanov, S. I.; Sidorov, L. N.; Yurovskaya, M. A.; Kemnitz, E. *New J. Chem.* **2007**, *72*, 89–93.
(47) Clare, B. W.; Kepert, D. L. *J. Mol. Struct. (Theochem)* **1999**, *491*, 249–264.
(48) Goryunkov, A. A.; Ioffe, I. N.; Kuvychko, I. V.; Yankova, T. S.; Markov, V. Y.; Streletskii, A. V.; Dick, D. L.; Sidorov, L. N.; Boltalina, O. V.; Strauss, S. H. *Fullerenes Nanotubes Carbon Nanostruct.* **2004**, *12*, 181–185.
(49) Troyanov, S. I.; Popov, A. A.; Denisenko, N. I.; Boltalina, O. V.; Sidorov, L. N.; Kemnitz, E. *Fullerenes Nanotubes Carbon Nanostruct.* **2003**, *11*, 61–77.
(50) Al-Matar, H.; Abdul-Sada, A. K.; Avent, A. G.; Fowler, P. W.; Hitchcock, P. B.; Rogers, K. M.; Taylor, R. *J. Chem. Soc., Perkin Trans. 2* **2002**, 53–58.
(51) Clare, B. W.; Kepert, D. L. *J. Mol. Struct. (Theochem)* **1995**, *340*, 125–142.

$C_3F_7)_2$ hexagons.[52] For *t*-Bu groups, isolated $C_6(X)$ hexagons were predicted to give rise to the most stable addition patterns.[44] In this case, placing bulky *t*-Bu groups on *para* cage C atoms is less stable than addition patterns with isolated C_6X hexagons.

The fullerene itself can place restrictions on the kinds and lengths of ribbons (or loops) of $C_6(X)_2$ hexagons that can be formed. In C_{60}, for example, a *ribbon* with more than three edge-sharing *p*-$C_6(X)_2$ hexagons is not possible, as shown in the Schlegel diagrams for 18 $C_{60}(CF_3)_n$ ($n = 2-12$) derivatives in Figure S-9 (Supporting Information). The DFT-predicted most stable isomers of $C_{60}(CF_3)_n$ with $n = 6$, 8, 10, and 12 have "a ribbon-of-edge-sharing $C_6(CF_3)_2$-hexagons" addition patterns that can be described as p^3mp-$C_{60}(CF_3)_6$ (p^3mp = *para-para-para-meta-para*),[48,53] p^3mp,p-$C_{60}(CF_3)_8$,[1] p^3mp,p^3-$C_{60}(CF_3)_{10}$,[1,54] and $(pm)^6$(loop)-$C_{60}(CF_3)_{12}$.[9] There are five other isomers of $C_{60}(CF_3)_{10}$ that have been isolated with DFT relative energies within 10 kJ mol^{-1} of the p^3mp,p^3 isomer, and these are $p^3mpmpmp$-,[55] pmp^3mpmp-,[7] p^3mpmp,p-,[1] $pmpmpmpmp$-,[1] and p^3m^2(loop),p^3m^2(loop)-$C_{60}(CF_3)_{10}$.[56] Five of the six $C_{60}(CF_3)_{10}$ isomers are asymmetric, as are the most stable isomers of $C_{60}(CF_3)_6$ and $C_{60}(CF_3)_8$, and this fact alerted fullerene theorists that they could no longer rely on symmetry to reduce the complexity of calculations on stable fullerene$(X)_n$ derivatives.

All (C_{60+x})[5,6] fullerenes have *x* C atoms known as triple-hexagon junctions (THJs). There are no examples of hollow fullerene$(X)_n$ compounds with substituents on THJs if $n < 38$, including $C_{76}Cl_{18}$[29] and two isomers of $C_{78}Br_{18}$[30] (the two $n = 38$ exceptions are $C_{70}F_{38}$[57] and $C_{74}F_{38}$[58]). This is almost certainly because THJs are the least pyramidal of all fullerene cage C atoms. A "pyramidal" figure of merit for fullerene C atoms has been defined as the π-orbital axis vector (POAV) angle, $\theta_{\sigma\pi}$,[16,59] and for simplicity we will use the angle $\theta_{\sigma\pi} - 90°$, hereinafter denoted θ_p. As points of reference, θ_p is 11.64° for DFT-optimized C_{60}, it ranges from 11.4(2)° to 11.9(2)° for the C_{60} molecule in C_{60}·Pt(OEP)·$2C_6H_6$,[26] and it ranges from 8.6° for the THJs in DFT-optimized C_{70} to 12.0° for the most pyramidal cage C atoms in C_{70}. Therefore, *all* IPR fullerenes have only 60 cage C atoms to which substituents can be added *if THJs are avoided*, regardless of how many C atoms are in the cage. This imposes a significant restriction on what addition patterns are likely to be found, especially with 12 or fewer substituents.

Despite this restriction, exohedral derivatives with ribbons or ribbon fragments longer than p^3 are possible for C_{70} and other HHFs. For the six isomers of $C_{70}(CF_3)_{10}$, the most stable addition pattern is C_1-p^7mp, followed closely in energy by the C_2-p^9 isomer (Schlegel diagrams for 17 $C_{70}(CF_3)_n$ derivatives with $n = 2-12$ are shown in Figure S-10 in the Supporting Information).[2,8] The first seven HHF$(CF_3)_n$ compounds that were isolated all have 12 CF_3 groups (one per pentagon) and contain seven different fullerene cage isomers (these are listed in Table 1).[17] Three of these, **74-12-1**,[15] **78-12-1**,[15] and **82-12-1**,[17] have C_2-p^{11} addition patterns. However, a p^{11} single-ribbon addition pattern is geometrically not possible for the other four cages of the seven isolated compounds *if THJs are avoided*. For example, **82-12-2**, with the C_{82}-$C_2(5)$ cage, has a double-ribbon p^5,p^5 addition pattern; **80-12-1**, with the C_{80}-$C_{2v}(5)$ cage, has a p^{10}(loop),*p* addition pattern; and **76-12-1**, with the C_{76}-$T_d(2)$ cage, has a p^9(loop),p^2 addition pattern.[17] The tendency for fullerene$(CF_3)_{12}$ derivatives to be among the most abundant fullerene$(CF_3)_n$ derivatives in many high-temperature reactions of bare-cage fullerenes with CF_3I may derive from the steric strain introduced by adding more than one bulky CF_3 group to a fullerene pentagon, although there are C_{60} derivatives with up to 18 CF_3 groups and two of the compounds reported in this paper have 14 CF_3 groups. Nevertheless, there are only three compounds with 1,3-$C_5(CF_3)_2$ pentagons *and* 12 or fewer CF_3 groups, out of a total of more than 60 well-characterized fullerene$(CF_3)_{n\le12}$ derivatives, and all three are C_{60} derivatives.[7,14,60] Furthermore, all six of the previously reported structurally characterized HHF$(CF_3)_n$ derivatives have "*para*-only" addition patterns. As will be seen, this tendency is quite general for HHF$(CF_3)_n$ derivatives with $n \le 12$, although the first example with a *m*-$C_6(CF_3)_2$ hexagon is one of the three X-ray structures reported in this work.

Finally, the many 1,2-cycloadditions to HHFs that have been studied support the early observation of Diederich and co-workers that the cage double bonds that tend to undergo cycloaddition first (i.e., the "most-reactive" double bonds) are those in which the C atoms are among the most pyramidal in the fullerene precursor (i.e., the cage C atoms with the largest θ_p angles).[32,33,61] This is true because these atoms are the most predisposed to undergo the change in hybridization from (nominally) C(sp^2) to C(sp^3). However, we recently noted that, for previously reported HHF$(X)_n$ derivatives with ribbons-or-loops-of-edge-sharing-*p*-$C_6(X)_2$-hexagon addition patterns, these double bonds remain intact.[18] In such derivatives, which now include 10 of the compounds reported in this work, the *most pyramidal* cage C atoms in the fullerene precursor *remain sp^2 hybridized*. This will be discussed in more detail in section III.B.3.

The terminology "most-reactive" bonds (or "most-reactive" cage C atoms) can be interpreted in a number of ways. These bonds are certainly the first to undergo 1,2-addition reactions in C_{70} and HHFs, but is that because the products are more stable than alternate structures, a thermodynamic effect, or because these bonds react faster with the addend reactant, a kinetic effect? To avoid any ambiguity in the discussion below, we will refer to the observed phenomena as "HHF addition-pattern principles" and not as "HHF reactivity principles". When DFT calculations predict that one addition pattern is thermodynamically more stable than another, this will be clearly indicated.

B. X-ray Crystallography. 1. General Comments. A displacement ellipsoid plot, a Schlegel diagram with the same orientation as the displacement ellipsoid plot, and a partially numbered ball-and-stick plot for **78-10-1**, **78-10-2**, and **78-12-2** are shown in Figures 5, 6, and 7, respectively (a larger and more

(52) Shustova, N. B.; Kuvychko, I. V.; Boltalina, O. V.; Strauss, S. H. *Acta Crystallogr.* **2007**, *E63*, o4575.
(53) Dorozhkin, E. I.; Goryunkov, A. A.; Ioffe, I. N.; Avdoshenko, S. M.; Markov, V. Y.; Tamm, N. B.; Ignat'eva, D. V.; Sidorov, L. N.; Troyanov, S., I. *Eur. J. Org. Chem.* **2007**, 5082–5094.
(54) Shustova, N. B.; Peryshkov, D. V.; Kareev, I. E.; Boltalina, O. V.; Strauss, S. H. *Acta Crystallogr.* **2007**, *E63*, o3398.
(55) Kareev, I. E.; Lebedkin, S. F.; Miller, S. M.; Anderson, O. P.; Strauss, S. H.; Boltalina, O. V. *Acta Crystallogr.* **2006**, *E62*, o1498−o1500.
(56) Kareev, I. E.; Lebedkin, S. F.; Popov, A. A.; Miller, S. M.; Anderson, O. P.; Strauss, S. H.; Boltalina, O. V. *Acta Crystallogr.* **2006**, *E62*, o1501−o1503.
(57) Hitchcock, P. B.; Avent, A. G.; Martsinovich, N.; Troshin, P. A.; Taylor, R. *Org. Lett.* **2005**, *7*, 1975–1978.
(58) Goryunkov, A. A.; Markov, V. Y.; Ioffe, I. N.; Sidorov, L. N.; Bolskar, R. D.; Diener, M. D.; Kuvychko, I. V.; Strauss, S. H.; Boltalina, O. V. *Angew. Chem., Int. Ed.* **2004**, *43*, 997–1000.
(59) Haddon, R. C. *Science* **1993**, *261*, 1545–1550.
(60) Shustova, N. B.; Anderson, O. P.; Boltalina, O. V.; Strauss, S. H.; Kareev, I. E. *Acta Crystallogr.* **2008**, *E64*, o0159.
(61) Herrmann, A.; Diederich, F.; Thilgen, C.; Ter Meer, H.-U.; Muller, W. H. *Helv. Chim. Acta* **1994**, *77*, 1689–1706.

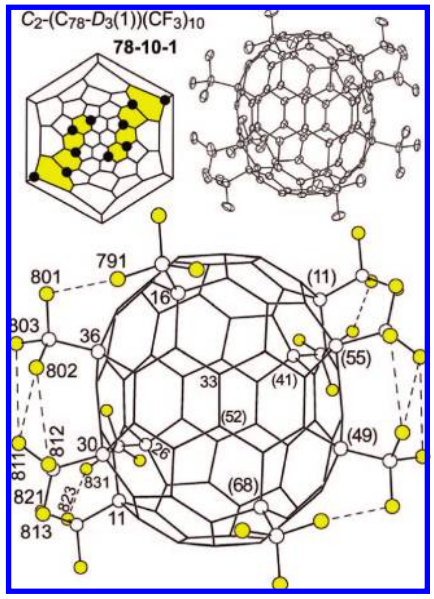

Figure 5. Drawings of the C_2 structure of **78-10-1** (50% probability ellipsoids in the upper drawing). The parent fullerene is C_{78}-D_3(1). A Schlegel diagram is also shown, with black circles representing the cage C atoms to which the 10 CF_3 groups are attached. The two ribbons of edge-sharing *p*-$C_6(CF_3)_2$ hexagons are highlighted. The two- and three-digit numbers in the lower drawing are C and F atom numbers, respectively (the cage C atom numbers are IUPAC lowest locants; F791 is bonded to C79, F802 is bonded to C80, etc.) The C atom numbers in parentheses are also IUPAC lowest locants, but since this molecule has crystallographic C_2 symmetry, IUPAC C68 = crystallographic C16′, IUPAC C49 = crystallographic C36′, etc. The lower drawing emphasizes the F···F interactions between pairs of mutually *para* CF_3 groups. The F···F distances and other structural parameters are listed in Table 3. The crystallographic C_2 axis passes through the bisector of the C33−C33′ bond (IUPAC C33−C52) and the centroid of the 23,24,25,23′,24′,25′ hexagon (IUPAC 23,24,25,44,43,42; see also Table S-3 in the Supporting Information).

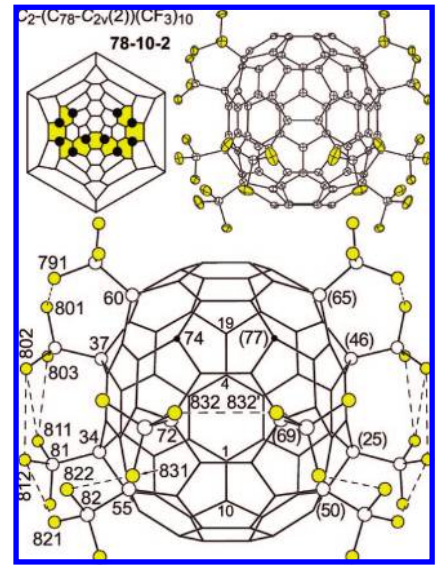

Figure 6. Drawings of the C_2 structure of **78-10-2** (50% probability ellipsoids in the upper drawing). The parent fullerene is C_{78}-C_{2v}(2). A Schlegel diagram is also shown, with black circles representing the cage C atoms to which the 10 CF_3 groups are attached. The ribbon of nine edge-sharing *p*-$C_6(CF_3)_2$ hexagons is highlighted. The two- and three-digit numbers in the lower drawing are C and F atom numbers, respectively; F791 is bonded to C79, F802 is bonded to C80, etc. The C atom numbers in parentheses are also IUPAC lowest locants, but since this molecule has crystallographic C_s symmetry, IUPAC C65 = crystallographic C60′, IUPAC C46 = crystallographic C37′, etc. This drawing emphasizes the F···F interactions between pairs of mutually *para* CF_3 groups. These distances and other structural parameters are listed in Table 3. The crystallographic symmetry plane includes C1, C4, C10, and C19 (see also Table S-3).

detailed displacement ellipsoid plot for each molecule, diagrams showing the complete atom numbering, and other information about the structures are available in the Supporting Information, including Figures S-11−S-13). Data collection and refinement parameters for the structures are listed in Table 2. Relevant interatomic distances and angles are listed in Table 3, including F···F distances between neighboring CF_3 groups (i.e., CF_3 groups that share the same hexagon). The structure of **78-10-1** represents the first X-ray structure of the C_{78}-D_3(1) cage. The structures of **78-10-2** and **78-12-2** represent the second X-ray structures of the C_{78}-C_{2v}(2) and C_{78}-C_{2v}(3) cages, respectively. The first X-ray structure of each was reported for a disordered solid solution of (C_{78}-C_{2v}(2))Br_{18} and (C_{78}-C_{2v}(3))Br_{18}.[30] Together with the published X-ray structure of C_2-p^{11}-(C_{78}-D_{3h}(5))$(CF_3)_{12}$,[15] four of the five possible IPR isomers of C_{78} have now been verified by X-ray crystallography.

2. X-ray Structure of 78-10-1. The 10 CF_3 groups in this molecule are arranged on two symmetry-related p^4 ribbons, giving an overall C_2-p^4,p^4 addition pattern. The estimated standard deviations (esd's) for individual cage C−C distances are 0.002−0.003 Å. The molecule has crystallographic C_2 symmetry (the C_2 axis is the only remaining symmetry element of bare-cage C_{78}-D_3(1)). Inspection of the Schlegel diagram for this derivative shows that a single-ribbon p^9 addition pattern is not possible if THJs are avoided (a larger, color-coded Schlegel diagram and other information about this structure are shown in Figures S-3 and S-11, respectively). Furthermore, the two p^4 ribbons cannot be extended to make a *stable* isomer of (C_{78}-D_3(1))$(CF_3)_{12}$ with two p^5 ribbons because the cage C atoms *para* to the terminal CF_3 groups on the p^4 ribbons either are THJs or are on pentagons that already have one CF_3 group (this is not the case with **82-12-1** and **84-12-3**, both of which have cages that allow a stable C_2-p^5,p^5 addition pattern to be formed). It is also not possible to make an isomer of (C_{78}-D_3(1))$(CF_3)_{12}$ by forming an additional *p*-$C_6(CF_3)_2$ hexagon elsewhere in the molecule, because the two remaining substituent-free pentagons on **78-10-1** are not adjacent to a common hexagon. It is possible that reasonably stable addition patterns for the composition $C_{78}(CF_3)_{12}$ with this cage may exist, but if so they are present in such small amounts in the mixtures of products that they have not yet been identified.

3. X-ray Structure of 78-10-2. The 10 CF_3 groups in this molecule are arranged on a single p^9 ribbon. The molecule has crystallographic C_s symmetry (only this mirror plane remains from the C_{78}-C_{2v}(2)) bare cage). Neither the molecule nor any of the CF_3 groups individually exhibits unusual librational motion. Most of the esd's for individual cage C−C bonds are 0.003 Å, several are 0.004 Å, and one is 0.005 Å.

As we have observed with many fullerene$(CF_3)_n$ compounds,[1,2] the DFT-optimized structure of **78-10-2** matches the X-ray structure in many important details, including the 68 unique cage C−C distances, the F_3C···CF_3 and F···F distances for mutually *para* CF_3 groups, and the F−C−C−C torsion angles that define the conformations of the CF_3 groups with respect to the fullerene cage. Relevant drawings are shown in Figure 8, and relevant parameters are listed in Table 3. (Similar drawings for **78-10-1** are shown in Figure S-14 in the Supporting Information.) For example, the C81 CF_3 group has a F813−C81−C34−C35 torsion angle of 21.5(1)° in the X-ray structure and 19.4° in the DFT structure (the CF_3 group would be fully

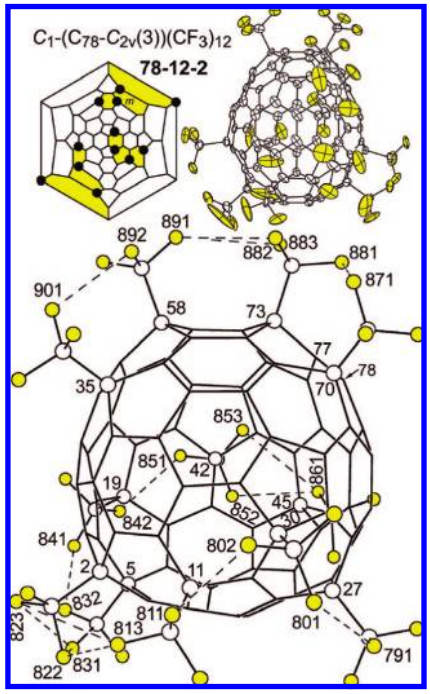

Figure 7. Drawings of the structure of asymmetric **78-12-2** (50% probability ellipsoids in the upper drawing). The parent fullerene is C_{78}-$C_{2v}(3)$. A Schlegel diagram is also shown (same orientation as the thermal ellipsoid plot), with black circles representing the cage C atoms to which the 10 CF_3 groups are attached. The two ribbons of edge-sharing $C_6(CF_3)_2$ hexagons are highlighted. One is a p^3 ribbon of four CF_3 groups, and one is a p^5mp ribbon of eight CF_3 groups. The two- and three-digit numbers in the lower drawing are C and F atom numbers, respectively (the cage C atom numbers are IUPAC lowest locants; F791 is bonded to C79, F802 is bonded to C80, etc.). The lower drawing emphasizes the F···F interactions between pairs of mutually *para* CF_3 groups and between the C80 and C81 CF_3 groups, which are *meta* to one another. The F···F distances and other structural parameters are listed in Table 3. The original C_2 axis of the parent fullerene, which is not present in this derivative, bisected the C77−C78 bond.

staggered if this angle were 60° and fully eclipsed if it were 0°), and the C80···C81 and C81···C82 distances are 3.739(3) and 4.074(3) Å, respectively, in the X-ray structure and 3.769 and 4.096 Å in the DFT structure. The consistently good agreement between more than 20 X-ray and DFT-optimized structures we have published provides confidence that the PBE functional and the TZ2P-quality basis set(s) we use accurately predict the structural parameters of fullerene$(CF_3)_n$ compounds that have not yet been characterized by single-crystal X-ray diffraction (as long as the proposed addition pattern is correct).

In line with the HHF addition-pattern principle we recently reported for **74-12-1**, **78-12-1**, **84-12-2**, $(C_{78}$-$C_{2v}(2))Br_{18}$, and $(C_{78}$-$C_{2v}(3))Br_{18}$,[18] and which we now report is also followed by the compounds **76-12-1**, **80-12-1**, **82-12-1**, and **82-12-2**,[17] the substituents in **78-10-1** and in **78-10-2** are *not* attached to cage C atoms that were the most pyramidal C atoms in the bare-cage fullerene precursor. This is shown graphically in Figure 9 for **78-10-2** and C_{2v}-$(C_{78}$-$C_{2v}(2))Br_{18}$ (see Figures S-15−S-20 in the Supporting Information for similar plots for **78-10-1** and for the other compounds listed in this paragraph). In fact, six of the cage C(sp^3) atoms in **78-10-2** did not have the largest *available* θ_p angles in the bare-cage precursor *even if* the interpentagonal C−C bond (ICCB) C atoms are set aside (the ICCB C atoms are those that make up the red C−C bonds in Figure 9). Specifically, there are four non-ICCB C(sp^2) atoms in **78-10-2** that had bare-cage θ_p angles of 11.2° (and two that had θ_p angles of 10.5°), whereas the six C(sp^3) atoms in question in **78-10-2** had bare-cage θ_p angles of only 10.3° or 10.4°. The ICCBs in C_{78}-$C_{2v}(2)$ are some of the shortest C−C bonds in the cage, and they remain some of the shortest bonds in **78-10-2** and C_{2v}-$(C_{78}$-$C_{2v}(2))Br_{18}$. For comparison, Table S-4 (Supporting Information) lists the X-ray and DFT ICCB distances for **78-10-2** and the DFT distances for C_{78}-$C_{2v}(2)$. Nine of the ICCBs are slightly longer in **78-10-2** than in the fullerene precursor, by an average of 0.009 Å, and eight are slightly shorter, by an average of 0.013 Å.

Why should large-θ_p-angle C atoms (i.e., ICCB C atoms) be the addition sites of choice for 1,2-additions but not for multiple 1,4-additions that produce ribbons or loops of edge-sharing p-$C_6(CF_3)_2$ hexagons? To begin to answer this question, we have started a computational study of $HHF(CF_3)_2$ derivatives of selected cages with all possible p-$C_6(CF_3)_2$ addition patterns. The complete results will be reported at a later time. Here we note that, for p-$C_6(CF_3)_2$ isomers of the hypothetical composition $(C_{78}$-$C_{2v}(3))(CF_3)_2$, the DFT-predicted lowest energy isomer (0.0 kJ mol^{-1} by definition) *does* have its two CF_3 groups on ICCB C atoms. Furthermore, the average relative energy of all isomers with CF_3 groups on two ICCB C atoms is 16 kJ mol^{-1}, while the average relative energy of all isomers with CF_3 groups on non-ICCB C atoms (not counting THJs) is 34 kJ mol^{-1}. This demonstrates that, if two and only two CF_3 groups are added to a higher fullerene, adding them to large-θ_p-angle C atoms is *not* intrinsically destabilizing. The underlying reason(s) for the new HHF addition-pattern principle exemplified by the plots in Figure 9 and in Figures S-15−S-20 must be found elsewhere.

We believe that one reason is that *long* ribbons of edge-sharing p-$C_6(CF_3)_2$ are not possible if ICCB C atoms are used, and longer ribbons apparently lead to a more stable $HHF(X)_n$ derivative than a larger number of short ribbons or isolated p-$C_6(CF_3)_2$ hexagons. For example, inspection of the Schlegel diagram for the C_{78}-$C_{2v}(2)$ cage in Figure 9 (ignoring the black circles) shows that the longest *para*-only ribbon would be p^3 if only ICCB C atoms were used. The cage C atom that is *para* to the ICCB C atom at either end of the hypothetical p^3 ribbon is a THJ, and putting substituents on THJs is not a realistic option for continuing a ribbon of edge-sharing $C_6(CF_3)_2$ hexagons in a *stable* derivative. In our preliminary study of *para*-hexagon isomers of $(C_{78}$-$C_{2v}(3))(CF_3)_2$, the lowest-energy isomer with one sp^3 THJ is 70 kJ mol^{-1} above the most stable isomer, and the average relative energy of all isomers with one sp^3 THJ is 96 kJ mol^{-1} (not surprisingly, isomers with two sp^3 THJs are even less stable). For the C_{78}-$D_3(1)$, C_{78}-$C_{2v}(3)$, and C_{78}-$D_{3h}(5)$ cages, the longest *para*-only ribbons with substituents confined to ICCB C atoms would be p^3, p^2, and p^1 (i.e., no ICCB ribbon is possible for C_{78}-$D_{3h}(5)$, only a p-$C_6(CF_3)_2$ hexagon), respectively (see Figures S-3, S-5, and S-16). In contrast, the longest *para*-only ribbons for these three cages if ICCB C atoms (and THJs) are avoided are p^4 (as in **78-10-1**), p^7 (as in the proposed structure for **78-8-1**; see below), and p^{11} (as in **78-12-1**), respectively.

Although there is only one p^9 ribbon possible for the C_{78}-$C_{2v}(2)$ cage (i.e., the C_s symmetry addition pattern found for **78-10-2**), there is another possible *para*-only addition pattern that is predicted to be reasonably stable for this cage. This is the C_2-p^4,p^4 addition pattern that we believe represents the structure of **78-10-3**. It will be discussed in more detail in the NMR section below, but here we note that its energy relative to the **78-10-2** addition pattern is 20 kJ mol^{-1}. This provides at least one benchmark for the difference in energy between a

Table 3. X-ray and DFT Distances (Å) and Angles (deg) and ^{19}F NMR $-\delta$ and J_{FF} Values for Fullerene$(CF_3)_n$ Compounds[a]

compd	multiplet[b]	$-\delta(^{19}F)$, ppm	F−C−C−C, deg[c]	$F_3C\cdots CF_3$, Å[d]	J_{FF}, Hz[e]	F···F, Å[f]	F−C···C−F, deg[g]
74-12-1[h]	**f** (q)	70.0	52.4 [52.0]	4.013 [3.962]	15.0	2.690 [2.633]	74.6 [75.1]
	b (as)	63.2	23.5 [24.8]	4.309 [4.213]	15.0, 13	2.741 [2.701]	51.8 [60.2]
	e (as)	67.7	54.0 [47.1]	4.053 4.024]	13, 12	2.864, 2.766 [2.879, 2.760]	55.0, 60.4 [48.8, 65.5]
	a (as)	55.2	1.0 [0.8]	4.042 [3.986]	12, 12	2.745, 2.853 [2.682; 2.808]	65.0, 50.3 [59.4, 56.1]
	d (um)	67.5	51.5 [56.4]	4.339 [4.313]	12, −	2.676 [2.622]	45.2 [62.9]
	c (um)	63.6	33.1 [33.6]	3.938 [3.875]	−	2.685 [2.639] (→ **c′**)	86.0 [87.4]
76-6-1[i]	**f** (q)	71.2	47.7	4.112	17.7	2.648	63.0
	a (um)	59.3	19.2	3.984	17.7, −	2.842, 2.951	90.5, 25.6
	c (as)	63.1	31.0	3.774	−, −	2.657, 2.923	94.9, 20.4
	b (um)	62.4	27.1	4.377	−, −	2.715	36.0
	d (as)	68.5	52.6	4.220	16.3, −	2.610	53.6
	e (q)	69.3	49.2	*4.220*	16.9	*2.610*	*53.6*
76-10-1[j]	**e** (q)	71.6	52.8	4.109	11.9	2.678	69.6
	a (as)	58.2	22.1	3.771	11.9, 16	2.700, 2.798	96.7, 20.2
	b (as)	64.4	31.0	4.386	16, 12	2.679	31.4
	c (as)	68.1	51.6	4.210	12, 16.3	2.606	55.1
	d (q)	70.3	49.0	*4.210*	16.3	*2.606*	*55.1*
76-12-2[k]	**f** (um)	73.3	58.7	4.576	≤5	2.899	4.7
	d (um)	67.6	45.9	3.863	≤5, −	2.606, 2.887	62.1, 51.9
	c (qq)	64.5	26.6	3.763	−, 14	2.647, 2.928	95.2, 18.7
	b (m)	60.2	27.5 {10.9}	3.977	14, 15	2.822, 3.054	91.6, 23.5
	a (m)	56.8	23.4 {52.2}	4.150	15, 20	2.631	59.4
	e (q)	70.6	52.9	*4.150*	20	*2.631*	*59.4*
78-8-1[l]	**d** (q)	70.1	51.8	4.089	16.1	2.675	66.4
	b (as)	63.6	32.3	4.246	16.1, −	2.817	40.7
	c (as)	65.6	29.3	4.034	−, −	2.732	56.3
	a (as)	61.2	35.9	4.200	−, −	2.741 (→ **a′**)	61.1
78-10-1[m]	**e** (q)	72.4	53.9 [52.0]	4.162 [4.142]	10.7	2.725 [2.678]	68.9 [67.1]
	a (um)	59.4	24.0 [29.0]	3.696 [3.654]	10.7, −	2.798; 2.669, 2.899 [2.685; 2.666, 2.895]	17.9; 99.3, 15.8 [15.9; 101.9, 13.4]
	b (um)	59.7	27.3 [21.0]	4.037 [4.020]	−, 9.7	2.801 [2.597]	88.5 [73.4]
	c (ad)	64.9	30.1 [47.4]	4.218 [4.244]	9.7, 19.3	2.597 [2.481]	48.7 [14.9]
	d (q)	70.0	53.2 [59.5]	*4.218 [4.244]*	19.3	*2.597 [2.481]*	*48.7 [14.9]*
78-10-2[n]	**e** (q)	71.9	54.3 [43.8]	4.188 [4.110]	11.3	2.698 [2.675]	63.4 [68.8]
	a (as)	58.0	21.6 [26.0]	3.769 [3.739]	11.3, 11	2.882; 2.717, 2.976 [2.903; 2.610, 2.938]	19.0; 17.1, 97.3 [17.2; 16.3, 96.5]
	b (qq)	59.4	19.4 [21.5]	4.096 [4.074]	11, −	2.819 [2.680]	75.1 [64.4]
	c (um)	62.0	34.6 [40.1]	3.924 [3.754]	−, −	2.653 [2.581]	82.6 [83.8]
	d (um)	65.5	35.0 [31.6]	4.336 [4.299]	−, −	2.659 [2.625] (→ **d′**)	26.2 [0.0]
78-10-3[o]	**e** (q)	70.0	54.2	4.194	11.3	2.711	61.9
	a (um)	57.4	21.9	3.768	−, −	2.712	97.4
	b (um	59.4	21.7	4.084	−, −	2.830	78.6
	c (um)	60.9	32.3	4.007	−, −	2.627	75.7
	d (um)	66.9	47.3	*4.007*	−, −	*2.627*	*75.7*
78-12-2[p]	**l** (q)	72.3	58.7 [57]	4.549 [4.47]	6.9	2.929 [2.85]	21.2 [21]
	h	66.3	35.8 [39]	3.822 [3.79]	6.9, 14	2.609 [2.58]	21.6 [15]
	d	63.6	57.2 [58]	4.038 [3.96]	14, 15	2.652, 2.953 [2.64, 2.79]	61.3, 53.3 [59, 56]
	b	59.1	14.6 [10]	4.056 [4.04]	15, 9	2.911, 3.067 [2.76, 2.96]	92.5, 21.1 [74, 39]
	c	62.7	29.2 [44]	4.092 [4.06]	9, 15	2.600 [2.39]	62.8 [17]
	g	65.3	52.4 [48]	4.284 [4.17]	15, 12	2.701 [2.63]	37.4 [52.8]
	f	64.5	15.7 [24]	4.028 [4.01]	12, 16.4	2.780, 2.909 [2.73, 3.07]	72.6, 43.6 [74, 37]
	k (q)	70.6	56.2 [53]	*4.028 [4.01]*	16.4	*2.780, 2.909 [2.73, 3.07]*	*72.6, 43.6 [74, 37]*
	i (q)	68.5	50.3 [49]	3.912 [3.83]	15.8	2.630 [2.59]	77.3 [76]
	a	56.4	11.2 [9]	4.055 [4.02]	15.8, 8	2.889, 2.902 [2.94, 2.96]	35.2, 81.1 [32, 84]
	e	64.4	35.1 [29]	4.021 [3.94]	8, 16.1	2.605 [2.62]	73.2 [76]
	j (q)	68.9	46.9 [48]	*4.021 [3.94]*	16.1	*2.605 [2.62]*	*73.2 [76]*
84-12-1[q]	**c** (q)	71.4	53.7	4.181	16.3	2.584; 2.853, 3.003	43.4; 48.7, 66.8
	b (q)	64.9	33.1	4.152	16.3, 12	2.787, 2.959; 2.746	50.7, 64.9; 62.1
	a (m)	61.5	26.2	4.028	12, −	2.729, 2.884 (→ **a′**)	62.0, 54.1
84-12-2[r]	**k** (q)	71.7	58.3 [50.4]	4.118 [4.166]	15−16[t]	2.903, 2.974 [2.568]	
	f (as)	66.0	11.9 [−][s]	4.223 [4.166]	16	2.728 [−][s]	[−]
	d (as)	64.0	58.6 [−][s]	3.962 [3.814]	16, 13	2.700, 2.752 [−][s]	[−]
	a (as)	56.5	7.3 [−][s]	3.959 [3.932]	13, 13	2.704, 2.782 [−][s]	
	e (as)	65.0	52.8 [59.8]	4.039 [3.988]	13, 11	2.794, 2.816 [2.716, 2.851]	
	c (as)	57.1	5.5 [6.0]	4.029 [3.997]	11, 13.6	2.742, 2.916 [2.676, 2.923]	
	h (q)	69.9	56.3 [58.1]	*4.029 [3.997]*	13.6		
	j (q)	71.5	53.0 [51.5]	4.012 [3.962]	10.9	2.720, 2.906 [2.678, 2.906]	
	b (um)	56.7	14.0 [14.1]	3.898 [3.846]	10.9, 15.0	2.665, 2.745 [2.648, 2.702]	
	g (q)	69.7	53.4 [49.5]	*3.898 [3.846]*	15.0	*2.665, 2.745*	

Table 3. Continued

compd	multiplet[b]	$-\delta(^{19}F)$, ppm	F−C−C−C, deg[c]	$F_3C\cdots CF_3$, Å[d]	J_{FF}, Hz[e]	F···F, Å[f]	F−C···C−F, deg[g]
						[2.648, 2.702]	
	i (q)	70.5	59.3 [59.1]	4.389 [4.331]	17.7	2.599 [2.535]	
	l (q)	71.7	58.9 [60.2]	*4.389 [4.331]*	ca. 17[t]	*2.599 [2.535]*	
84-12-3[u]	**f** (q)	71.3 {71.4}[v]	53.5 {53.7}[v]	4.177 {4.181}[v]	16.2	2.583; 2.850, 3.003 {2.584; 2.853, 3.003}[v]	44.5; 48.0, 67.5 {43.4; 48.7, 66.8}[v]
	d (um)	64.3 {64.9}	33.1 {33.1}	4.156 {4.152}	16.2, −	2.773, 2.980; 2.738 {2.787, 2.959; 2.746}	50.2, 65.3; 60.5 {50.7, 64.9; 62.1}
	a (um)	61.3 {61.5}	26.5 {26.2}	4.032 {4.028}	−, −	2.734, 2.877 (→ **a′**) {2.729, 2.884 (→ **a′**)}	60.7, 55.5 {62.0, 54.1}
	e (q)	70.1	52.0	4.084	15.1	2.566; 2.760, 2.927	57.2; 47.8, 68.4
	b (um)	61.4	29.9	4.161	15.1, −	2.807; 2.785, 3.298	40.0; 65.4, 46.5
	c (um)	63.6	27.5	4.070	−, −	2.713, 3.009 (→ **c′**)	59.3, 78.2
90-12-2[w]	**h** (q)	71.0	53.8	4.204	14.9	2.676	52.8
	b (um)	57.8	24.4	3.946	14.9; −	2.741, 2.767	80.2, 36.3
	e (um)	65.1	30.8	3.985	−, −	2.710, 2.802	51.5, 65.4
	c (um)	60.4	28.2	4.007	−, −	2.782, 2.792	46.8, 69.7
	d (um)	60.5	29.5	4.283	−, −	2.684	44.2
	f (um)	66.4	53.2	3.970	−, −	2.703, 2.803	63.8, 52.7
	a (um)	53.9	8.8	3.928	−; 13.2	2.699, 2.745	79.3, 37.1
	g (q)	69.8	53.3	*3.928*	13.2	*2.699, 2.745*	*79.3, 37.1*
	j (q)	72.5	59.8	4.500	11	2.738	1.7
	i (q)	72.2	59.2	*4.500*	11	*2.738*	*1.7*
	l (q)	73.2	60.0	4.603	6	2.893	2.6
	k (q)	73.0	59.2	*4.603*	6	*2.893*	*2.6*

[a] All data from this work except for **74-12-1** (C_2-p^{11}-(C_{74}-D_{3h}(1))$(CF_3)_{12}$; refs 15 and 17), **78-12-2** (C_1-p^5mp,p^3-(C_{78}-C_{2v}(3))$(CF_3)_{12}$; ref 17), and **84-12-2** (C_1-p^6,p^2,*p*-(C_{84}-C_2(11))$(CF_3)_{12}$; ref 18); values from X-ray structures are in square brackets; values in braces given with the values for **84-12-3** are the values for **84-12-1** for comparison; chloroform-*d* solutions at 24 ± 1 °C; C_6F_6 internal standard (δ −164.9); see Table 1 for IUPAC locants. [b] Abbreviations: q, quartet; qq, quartet of quartets; as, apparent septet; ad, apparent non-Pascal dectet with ca. 1:3:6:10:12:12:10:6:3:1 intensity pattern; m, complex multiplet; um, unresolved broad-envelope multiplet. [c] The smallest torsion angle for a CF_3 group between one of its C−F vectors and the cage hexagon−hexagon junction C−C vector to which the CF_3 group is attached. [d] The distance between the C atoms of CF_3 groups that share the same hexagon. [e] Coupling constants are known to ±0.2 Hz for terminal CF_3 quartets except when second-order effects result in a multiplet that is significantly different than a Pascal 1:3:3:1 quartet. In those case, the J_{FF} values are ca. ±1 Hz. Resonances for other CF_3 groups are multiplets; J_{FF} values for the ones that are apparent (but not true) septets are ±1 Hz; J_{FF} values for multiplets deconvoluted by spectral simulation are ±1 Hz. [f] Distance(s) between the F atoms of CF_3 groups that share the same hexagon. [g] Torsion angle(s) between C−F vectors of CF_3 groups that share the same hexagon. [h] C_2-p^{11}-(C_{74}-D_{3h}(1))$(CF_3)_{12}$; the ribbon/multiplet sequence is **f**−**b**−**e**−**a**−**d**−**c**−**c′**− etc.; the X-ray C···C, F···F, and torsion angle esd's are 0.002 Å, 0.002 Å, and 0.1°, respectively. [i] C_1-p^5-(C_{76}-D_2(1))$(CF_3)_6$; the ribbon/multiplet sequence is **f**−**a**−**c**−**b**−**d**−**e**. [j] C_2-p^4,p^4-(C_{76}-D_2(1))$(CF_3)_{10}$; the ribbon/multiplet sequence is **e**−**a**−**b**−**c**−**d**. [k] C_2-p^3mp,p^3mp-(C_{76}-D_2(1))$(CF_3)_{12}$; the ribbon/multiplet sequence is **f**−**d**−**c**−**b**−**a**−**e**; the two F−C−C−C torsion angles in braces are the values for an alternative isomer with the same type of addition pattern (i.e., a different C_2-p^3mp, p^3mp isomer) and a slightly higher energy (see text and Supporting Information for more details). [l] C_2-p^7-(C_{78}-C_{2v}(3))$(CF_3)_8$; the ribbon/multiplet sequence is **d**−**b**−**c**−**a**−**a′**− etc. The DFT-optimized structural parameters are the average of two nearly equienergetic sets of CF_3 conformations. [m] C_2-p^4,p^4-(C_{78}-D_3(1))$(CF_3)_{10}$; the ribbon/multiplet sequence is **e**−**a**−**b**−**c**−**d**; the X-ray C···C, F···F, and torsion angle esd's are 0.003 Å, 0.002 Å, and 0.2°, respectively. [n] C_s-p^9-(C_{78}-C_{2v}(2))$(CF_3)_{10}$; the ribbon/multiplet sequence is **e**−**a**−**b**−**c**−**d**−**d′**− etc.; the X-ray C···C, F···F, and torsion angle esd's are 0.003 Å, 0.003 Å, and 0.2°, respectively. [o] C_2-p^4,p^4-(C_{78}-C_{2v}(3))$(CF_3)_{10}$; the ribbon/multiplet sequence is **e**−**a**−**b**−**c**−**d**. [p] C_1-p^5mp,p^3-(C_{78}-C_{2v}(3))$(CF_3)_{12}$; the ribbon/multiplet sequences are **l**−**h**−**d**−**b**−**c**−**g**−**f**−**k** and **j**−**c**−**a**−**i**; the X-ray C···C, F···F, and torsion angle esd's are 0.008 Å, 0.007 Å, and 0.6°, respectively. [q] D_2-p^5,p^5-(C_{84}-D_2(22))$(CF_3)_{12}$; the ribbon/multiplet sequence is **c**−**b**−**a**−**a′**− etc. [r] C_1-p^5,p^2,*p*-(C_{84}-C_2(11))$(CF_3)_{12}$, ref 18; the ribbon/multiplet sequences are **k**−**f**−**d**−**a**−**e**−**c**−**h**, **j**−**b**−**g**, and **i**−**l**. [s] This is an apparent J_{FF} value only, representing the average of 17.7 and 15.0 Hz for two quartets that are accidentally isochronous. [t] The X-ray torsion angles and F···F distances for multiplets **f**, **d**, and **a** are not given because the CF_3 group that gives rise to multiplet **d** is disordered in the solid state. [u] C_2-p^5,p^5-(C_{84}-D_2(22))$(CF_3)_{12}$; the ribbon/multiplet sequences are **f**−**d**−**a**−**a′**− etc. and **e**−**b**−**c**−**c′**− etc. [v] For comparison, the values in braces are the DFT-optimized values for **84-12-1**. One of the two ribbons in **84-12-3** is identical to both of the ribbons in **84-12-1**. [w] C_1-p^7,*p*,*p*-(C_{90}-C_1(32))$(CF_3)_{12}$; the ribbon/multiplet, sequences are **h**−**b**−**e**−**c**−**d**−**f**−**a**−**g**, **j**−**i**, and **l**−**k**.

single-ribbon p^{n-1} structure and a two-ribbon $p^{(n-2)/2}$,$p^{(n-2)/2}$ structure for an $HHF(X)_n$ derivative.

The stability of the fullerene π system that remains after an addition reaction has been carried out is undoubtedly an important factor in determining the relative thermodynamic stability of an $HHF(X)_n$ isomer. We are also investigating this factor in our ongoing computational study and will publish the results in due course. At this time, we will not speculate on the relative importance of the possible steric and electronic factors. Here we are demonstrating that there is a *general tendency* for $HHF(X)_n$ compounds with bulky X groups (i) to have addition patterns that are p^{n-1} ribbons, two $p^{(n-2)/2}$ ribbons, all-*para* loops, or some combination of all-*para* ribbons and/or loops of varying length depending on the geometric constraints of the parent fullerene, and (ii) to not have ICCB C(sp^3) atoms (and, of course, to not have sp^3 THJs). This is what we and others should refer to as the new HHF addition-pattern principle. It is a principle, not an inviolable rule. Exceptions can be expected. In fact, the first compound we have found that violates the new principle will be discussed next.

4. Structure of 78-12-2. The 12 CF_3 groups in this asymmetric molecule are arranged on two ribbons on the C_{78}-C_{2v}(3) cage, a short p^3 ribbon and a longer p^5mp ribbon. Some of the CF_3 groups exhibit significantly more librational motion than the others or than the CF_3 groups in **78-10-1** and **78-10-2**. Most of the esd's for individual cage C−C bonds are 0.008 Å, and several are 0.009 Å. Despite the lower precision of this structure compared with those for **78-10-1** and **78-10-2**, the agreement between the distances and angles listed in Table 3 for the X-ray and DFT structures of **78-12-2** is quite good (see also Figure S-13).

The most interesting aspect of this particular $HHF(CF_3)_n$ derivative is that it is the first to include a *m*-$C_6(X)_2$ hexagon *and* the first to have a ribbon addition pattern with ICCB C(sp^3) atoms (these addition-pattern features are related). This is shown in the θ_p plot in Figure 10. Note that all but six of the 26 ICCB

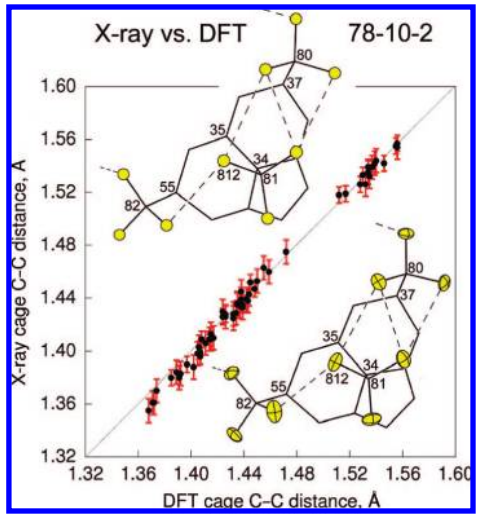

Figure 8. Comparisons of the X-ray and DFT-optimized structures of **78-10-2**. The error bars in the plot are $\pm 3\sigma$. The drawings show part of the p^9 ribbon of edge-sharing $C_6(CF_3)_2$ hexagons (the upper drawing is the DFT structure and the lower drawing is the X-ray structure; 50% probability ellipsoids for the F atoms shown). Note that the conformations of the CF_3 groups with respect to the fullerene cage are very similar in the two structures.

C atoms in **78-12-2** had bare-cage θ_p values greater than or equal to 11.4° and all but four of the 12 C(sp^3) atoms in **78-12-2** had bare-cage θ_p values less than or equal to 10.6°. A θ_p plot for C_{2v}-(C_{78}-C_{2v}(3))Br_{18}, which has the same cage as **78-12-2**, is also shown in Figure 10. None of the Br atoms are attached to ICCB C atoms. In contrast to the situation with **78-10-2** and C_{2v}-(C_{78}-C_{2v}(2))Br_{18}, which had 10 cage C(sp^3) atoms in common, only four cage C(sp^3) atoms are common to **78-12-2** and C_{2v}-(C_{78}-C_{2v}(3))Br_{18}.

Given that **78-12-2** is the most abundant HHF$(CF_3)_n$ derivative in the mixture of products prepared at 520−550 °C, it is quite possible that its addition pattern is especially stable. To begin to test this hypothesis, we compared its DFT-predicted energy to those of two alternative isomers with *para*-only ribbons and/or isolated *p*-$C_6(CF_3)_2$ hexagons, a p^7,*p*,*p* isomer and a p^5,p^2,p^2 isomer (see Figure S-21 in the Supporting Information). In both cases, the p^5mp,p^3 addition pattern was more stable by at least 45 kJ mol^{-1}. Although the structures shown in Figure S-21 are not the only possible *para*-only isomers of the composition (C_{78}-C_{2v}(3))$(CF_3)_{12}$, these results demonstrate that an HHF$(CF_3)_n$ addition pattern with a *meta*-$C_6(CF_3)_2$ hexagon can be more stable than at least some *para*-only addition patterns with the same fullerene cage. The new HHF addition-pattern principle, which is a good *initial* guide for predicting stable and/or likely addition patterns for HHF$(X)_n$ compounds when X is sterically bulky, does have exceptions (two more exceptions will be discussed below). We will continue to investigate, computationally and experimentally, the kinetic and thermodynamic factors that determine all fullerene$(CF_3)_n$ addition patterns.

C. Fluorine-19 NMR Spectra and DFT-Optimized Proposed Structures of HHF$(CF_3)_n$Compounds. 1. General Comments. Fluorine-19 NMR chemical shifts, coupling constants, and either 2D COSY correlations or unambiguous J_{FF} pairings are listed in Tables 3 and 4 for the 21 new HHF$(CF_3)_n$ compounds reported in this work. The NMR parameters for **78-12-2** were reported previously but are included in Table 3 so that correlations can be seen between NMR parameters and the

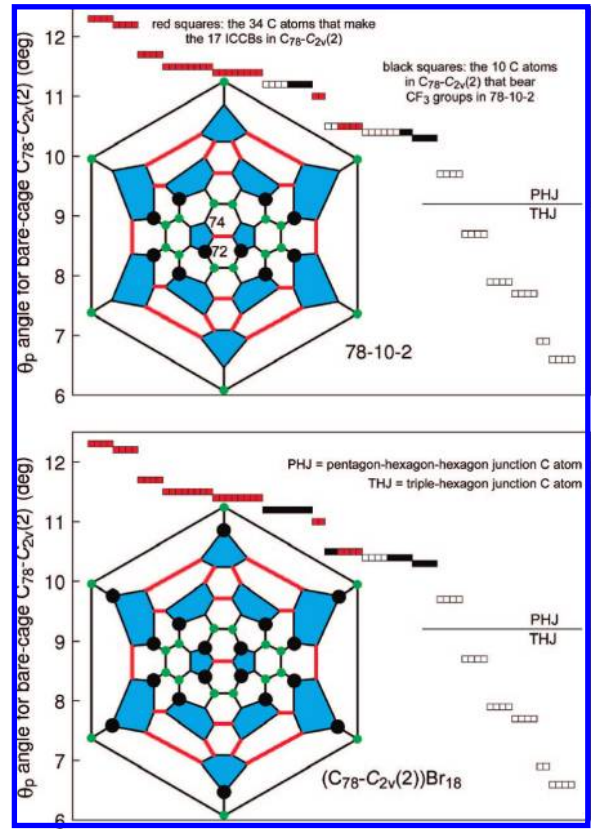

Figure 9. Color-coded Schlegel diagrams for C_s-p^9-(C_{78}-C_{2v}(2))$(CF_3)_{10}$ (**78-10-2**) and C_{2v}-(C_{78}-C_{2v}(2))Br_{18} and plots of θ_p angles for the cage C atoms in DFT-optimized C_{78}-C_{2v}(2). The 12 pentagons in the Schlegel diagrams are highlighted in blue, the 17 interpentagonal C−C bonds (ICCBs) are highlighted in red, cage C(sp^3) atoms are large black circles, and THJs are small green circles. The red and black squares in the θ_p plots represent ICCB C atoms and C(sp^3) atoms, respectively. Carbon atoms 72 and 74 are specifically indicated in the **78-10-2** Schlegel diagram to facilitate the discussion in the NMR section.

X-ray and DFT structures reported in this work. In addition, the previously reported compounds **74-12-1**[15] and **84-12-2**[18] are also included in Table 3 because their X-ray structures are two of the most precise fullerene structures available (cage C−C distance esd's ≤ 0.002 Å for **74-12-1** and 0.003 Å for **84-12-2**). The comparison of X-ray and DFT structural parameters such as F···F and F_3C···CF_3 distances and F−C−C−C and F−C···C−F torsion angles is necessary in order to correlate NMR data with DFT-optimized potential structures in the absence of an X-ray crystal structure determination. For example, in our previous work, we found that $^6J_{FF}$ and $^7J_{FF}$ values for *m*-$C_6(CF_3)_2$ and *p*-$C_6(CF_3)_2$ hexagons, respectively, depend upon the F···F distance between the CF_3 groups and on the F−C···C−F torsion angle (shorter distances and larger torsion angles lead to larger J_{FF} values),[1,2,13,17,62] and ^{19}F NMR $-\delta$ values for CF_3 multiplets are less than 60 ppm only when the corresponding CF_3 groups are eclipsed or nearly eclipsed.[7,17,63]

The 1D and 2D COSY ^{19}F NMR spectra and the X-ray and DFT structures of **84-12-2** will be used to illustrate these points.[18] This compound was chosen for a comparison because

(62) Kareev, I. E.; Santiso-Quinones, G.; Kuvychko, I. V.; Ioffe, I. N.; Goldt, I. V.; Lebedkin, S. F.; Seppelt, K.; Strauss, S. H.; Boltalina, O. V. *J. Am. Chem. Soc.* **2005**, *127*, 11497–11504.
(63) Kareev, I. E.; Lebedkin, S. F.; Bubnov, V. P.; Yagubskii, E. B.; Ioffe, I. N.; Khavrel, P. A.; Kuvychko, I. V.; Strauss, S. H.; Boltalina, O. V. *Angew. Chem., Int. Ed.* **2005**, *44*, 1846–1849.

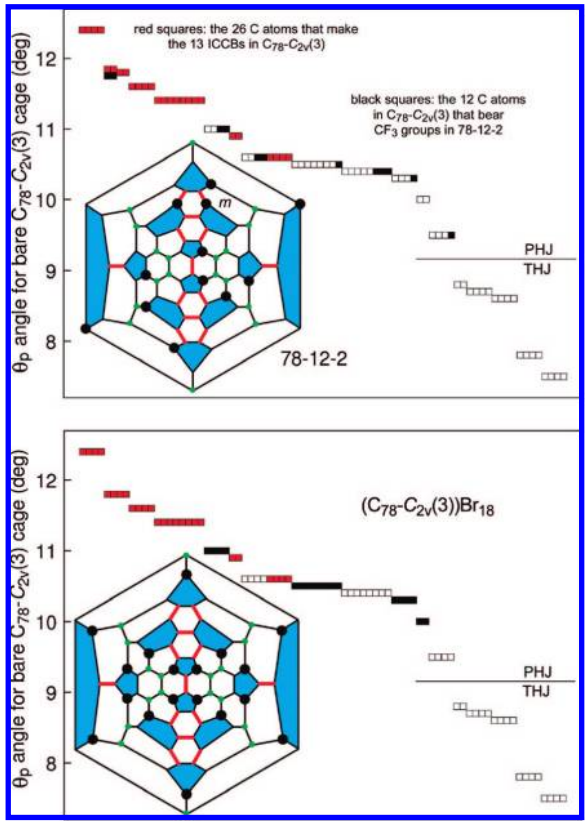

Figure 10. Color-coded Schlegel diagrams for C_1-p^5mp,p^3-(C_{78}-C_{2v}(3))$(CF_3)_{12}$ (**78-12-2**) and C_{2v}-C_{78}-(C_{2v}(3))Br_{18} and plots of θ_p angles for the cage C atoms in DFT-optimized C_{78}-C_{2v}(3). The 12 pentagons in the Schlegel diagrams are highlighted in blue, the 13 interpentagonal C−C bonds (ICCBs) are highlighted in red, cage C(sp^3) atoms are large black circles, and THJs are small green circles. The *m*-$C_6(CF_3)_2$ hexagon in **78-12-2** is indicated with the letter *m*. Note that two red squares represent the same cage C atoms as two black squares in the **78-12-2** θ_p plot.

it is asymmetric and therefore offers twice as many individual NMR vs structure correlations than any other HHF$(CF_3)_n$ derivative for which an X-ray structure has been reported, with the exception of **78-12-2** (and the X-ray structure of **84-12-2** is much more precise than the X-ray structure of **78-12-2**). The ^{19}F NMR spectrum of **84-12-2** is shown in Figure 11. The fact that the sample was 95+% pure (i.e., 95+ mol % of a single composition and a single isomer of that composition) can be readily seen. The 2D COSY spectrum, shown in Figure S-22 (Supporting Information), demonstrates that the compound has a ribbon of seven CF_3 groups, a ribbon of three CF_3 groups, and an isolated *p*-$C_6(CF_3)_2$ hexagon because there are six quartets, assigned to the CF_3 groups that share only one hexagon with another CF_3 group (i.e., the "terminal" CF_3 groups at the ends of each ribbon or on the isolated $C_6(CF_3)_2$ hexagon), and six quartets-of-quartets, assigned to the CF_3 groups that share two different hexagons with one CF_3 group each (i.e., the "internal" CF_3 groups on each ribbon). There are three multiplets, **a**, **b**, and **c**, with $-\delta$ values less than 60, so there should be three CF_3 groups that are nearly eclipsed on the ribbons. Inspection of Table 3 reveals that the middle CF_3 group on the ribbon of three, which gives rise to multiplet **b**, has DFT and X-ray F−C−C−C torsion angles of 14.0° and 14.1(1)°, respectively, as shown in the fragment of the X-ray structure shown in Figure 11 (this angle would be 0° is the CF_3 group were perfectly eclipsed). The expansion of multiplet **b** in Figure 11 demonstrates that it is possible to extract two J_{FF} values to at least ±1 Hz by trial-and-error spectral simulation for some of the quartets-of-quartets. In the case of multiplet **b**, it was known that the two coupling constants were 10.9 and 15.0 Hz because this CF_3 group is coupled to two terminal CF_3 groups, and the single J_{FF} value for each quartet is known to ±0.2 Hz (the J_{FF} values used for the simulation were 11 and 15 Hz). Finally, it is possible to assign the two ends of each ribbon by correlating the terminal J_{FF} values with the two sets of F···F distances and F−C···C−F torsion angles. In the case of the **j**−**b**−**g** p^2 ribbon, for example, we know that the C85 CF_3 group gives rise to multiplet **j** with $^7J_{FF}$ = 10.9 Hz instead of multiplet **g** with $^7J_{FF}$ = 15.0 Hz because the F851···F861 and F851···F863 distances, at 2.678(2) and 2.906(2) Å, are longer than the F871···F862 and F871···F863 distances of 2.648(2) and 2.702(2) Å. See Figures S-23 and S-24 (Supporting Information) for the 2D COSY ^{19}F NMR spectrum and similar structural drawings for **78-12-2**.

2. Addition Pattern of 76-10-1. In 2006, we reported the first example of a derivative of the insoluble C_{76}-T_d(2) cage, **76-12-1**.[17] However, since all of the $C_{76}(CF_3)_n$ compounds isolated in this work came from a mixture of *soluble* HHFs, the new $C_{76}(CF_3)_n$ compounds listed in Tables 3 and 4 almost certainly have the only other C_{76} IPR cage, viz. C_{76}-D_2(1).[15] Therefore, the overall symmetry of these compounds can only be D_2, C_2, or C_1. The ^{19}F NMR spectrum of **76-10-1** consists of five multiplets, two quartets, and three quartets-of-quartets. A 2D COSY spectrum was not necessary, because simulations of the multiplets allowed all four J_{FF} values, and hence the ribbon sequence, to be determined. The unusual structure of **78-12-2** notwithstanding, we tentatively assumed that the most likely structure of **76-10-1** would have a C_2-p^4,p^4 addition pattern with no *m*-$C_6(CF_3)_2$ hexagons, no ICCB C(sp^3) atoms, and no sp^3 THJs, and the lowest energy structure that fits these criteria is shown as a color-coded Schlegel diagram in Figure 12 (along with Schlegel diagrams for the proposed structures of **78-10-3**, **84-12-1**, **84-12-3**, and **90-12-2**, which will be discussed below). The IUPAC lowest locants and DFT-predicted HOMO−LUMO gap for **76-10-1** are listed in Table 1. Note that the positions *para* to the cage C(sp^3) atoms bearing the terminal CF_3 groups are THJs, ruling out a C_2-p^5,p^5 addition pattern for **76-12-2** (see below). Recall that if CF_3 groups were added only to ICCB C atoms, the longest *para*-only ribbon that could be formed before encountering a THJ would be p^3. The proposed structure has DFT-predicted terminal F···F distances of 2.678 and 2.606 Å, which correlate very well with the observed quartet J_{FF} values of 11.9 and 16.3 Hz, respectively. Furthermore, there is a CF_3 group that is second in each ribbon that has a $-\delta$ value of 58.2, and the smallest F−C−C−C torsion angle in the DFT-optimized structure, 22.1°, is for a CF_3 group that is second in each ribbon. There are three other possible C_2-p^4,p^4 isomers and 11 possible C_2-p^2mp,p^2mp isomers that would give rise to a five-multiplet ^{19}F NMR spectrum, and these are shown as Schlegel diagrams in Figure S-23. All of them have DFT-relative energies at least 80 kJ mol^{-1} higher than the proposed isomer (the relative energy of which is defined as 0.0 kJ mol^{-1}), and the two that are closest in energy to the proposed isomer, at 80.3 and 87.9 kJ mol^{-1}, also have unreasonably small HOMO−LUMO gaps of 0.45 and 1.01 eV, respectively. We also checked a number of C_2-(p^2-*p*),(p^2-*p*) pseudo-ribbon isomers, where the p^2 and *p* fragments are linked through a common 1,3-$C_5(CF_3)_2$ pentagon. For this set of isomers (not shown), the lowest energy is ca. 100 kJ mol^{-1} higher than that for the proposed structure. Therefore, in the

Table 4. Fluorine-19 NMR Data for New $HHF(CF_3)_n$ Compounds Not Listed in Table 3[a]

compd	multiplet (left to right in spectrum)/$-\delta/J_{FF}$, Hz/COSY correlations or visually obvious J_{FF} pairings													
76-8-1	**a**	**b**	**c**	**d**	**e**[b]	**f**[b]	**g**[b]	**h**[b]						
$-\delta$	59.8	63.0	63.0	68.9	70.2	70.6	71.4	71.7						
J_{FF}					16.6	17.3	8	8						
pairings							**h**	**g**						
76-8-2	**a**	**b**	**c**	**d**	**e**[b]	**f**[b]	**g**[b]	**h**[b]						
$-\delta$	59.0	61.3	64.0	68.8	69.6	71.0	71.2	71.5						
J_{FF}					17.3	16.9	15	15						
pairings							**h**	**g**						
76-10-2	**a**	**b**	**c**	**d**	**e**[b]	**f**[b]	**g**[b]	**h**[b]	**i**[b]	**j**[b]				
$-\delta$	59.4	61.4	63.6	68.5	69.6	70.9	71.8	72.0	72.2	72.3				
J_{FF}	11,17.6	9,16.6	11,13	9,13	17.6	16.6	9	13	13	9				
pairings	**c**,**e**	**d**,**f**	**a**,**d**	**b**,**c**	**a**	**b**	**j**	**i**	**h**	**g**				
76-10-3	**a**	**b**	**c**	**d**	**e**[b]	**f**[b]	**g**[b]	**h**[b]	**i**[b]	**j**[b]				
$-\delta$	59.1	60.9	63.7	69.4	69.7	70.0	71.2	71.9	72.1	72.3				
J_{FF}					16.6	14.3	16.6	6	15.1	6				
pairings					**g**		**e**	**j**		**h**				
76-10-4	**a**	**b**	**c**	**d**[b]	**e**[b]	**f**	**g**[b]	**h**[b]	**i**[b]	**j**[b]				
$-\delta$	57.3	59.0	63.4	67.5	68.6	69.9	70.4	71.7	72.9	73.0				
J_{FF}				15.1	11.3		18.4	12.4	10.5	5.2				
76-10-5	**a**	**b**	**c**	**d**[b]	**e**	**f**[b]	**g**[b]	**h**[b]	**i**[b]	**j**[b]				
$-\delta$	57.6	64.5	68.0	68.5	68.7	69.1	69.8	70.9	71.1	72.2				
J_{FF}				13.9		17.3	17.3	15.4	11.7	11.7				
pairings						**g**	**f**		**j**	**i**				
78-14-1[c]	**a**	**b**	**c**	**d**	**e**	**f**	**g**	**h**	**i**	**j**	**k**[b]	**l**[b]	**m**[b]	**n**[b]
$-\delta$	58.0	58.4	58.5	62.4	62.7	62.9	63.2	66.9	67.1	67.4	68.9	69.1	69.7	71.2
J_{FF}	12.8	um	um	13	um	um	ca. 12	um	12.6	12.4	14[q]	14[q]	13.9	7.5
COSY	**i**,**j**	**g**,**l**	**e**,**k**	**g**,**i**	**c**,**f**	**e**,**j**	**b**,**d**	**m**,**n**	**a**,**d**	**a**,**f**	**c**	**b**	**h**	**h**
84-10-1	**a**	**b**	**c**	**d**	**e**	**f**	**g**[b]	**h**[b]	**i**[b]	**j**[b]				
$-\delta$	56.5	56.7	62.7	63.0	63.2	64.4	69.1	70.0	70.1	71.9				
J_{FF}	12−13	12−13	14.5	≤14	≤14	13.0	16.1	16.3	15.4	15.3				
pairings	**d**,**f**	**e**,**f**	**d**,**e**	**a**,**c**	**b**,**c**	**a**,**b**	**h**	**g**	**j**	**i**				
84-14-1	**a**	**b**	**c**	**d**	**e**	**f**	**g**	**h**	**i**	**j**	**k**[b]	**l**[b]	**m**[b]	**n**[b]
$-\delta$	57.0	57.8	60.2	60.8	61.7	61.9	63.5	64.0	66.1	66.2	70.3	70.6	71.0	72.2
J_{FF}								um			16.2	16.9	13.6	10−11
90-12-1	**a**	**b**	**c**	**d**	**e**[b]	**f**[b]	**g**[b]	**h**[b]	**i**[b]	**j**[b]	**k**[b]	**l**[b]		
$-\delta$	55.8	56.4	57.8	65.3	69.1	72.2	72.2	72.6	72.6	72.7	72.8	73.3		
J_{FF}					14.9	−	−	−	11	11	6	6		
pairings									**j**	**i**	**l**	**k**		

[a] All data from this work; chloroform-*d* solutions at 24 ± 1 °C; C_6F_6 internal standard (δ −164.9). Coupling constants are known to ±0.2 Hz for terminal CF_3 quartets except when second-order effects result in a multiplet that is significantly different than a Pascal 1:3:3:1 quartet. In those case, the J_{FF} values are ca. ±1 Hz. Resonances for other CF_3 groups are multiplets; J_{FF} values for the ones that are apparent (but not true) septets are ±1 Hz; J_{FF} values for multiplets deconvoluted by spectral simulation are ±1 Hz. [b] Terminal CF_3 group on a ribbon of edge-sharing $C_6(CF_3)_2$ hexagons on the fullerene surface. [c] C_1-$C_{78}(CF_3)_{14}$; the ribbon/multiplet sequences are **n**−**h**−**m** and **l**−**b**−**g**−**d**−**i**−**a**−**j**−**f**−**e**−**c**−**k**.

absence of an X-ray structure, we believe that the addition pattern shown in Figures 1 and 12 is the most likely structure of **76-10-1**.

3. Addition Pattern of 76-12-2. The ^{19}F NMR spectrum of **76-12-2** consists of six multiplets, two quartets, and four quartet-of-quartets. One of the quartets has an unusually small J_{FF} value of 5(1) Hz (i.e., unusually small for fullerene$(CF_3)_n$ compounds[1,2,7,13]). The NMR spectrum requires overall C_2 symmetry and two ribbons of six J_{FF}-coupled CF_3 groups, most likely on five edge-sharing $C_6(CF_3)_2$ hexagons. As stated above, two symmetry-related p^5 ribbons are not possible for the C_{76}-$D(1)$ cage if THJs are not to be used. It is much more likely that this compound has two p^3mp ribbons, with each ribbon having two of the six CF_3 groups attached to ICCB $C(sp^3)$ atoms due to the presence of the *m*-$C_6(CF_3)_2$ hexagon, a type of addition pattern we would not have proposed as "most likely" before the X-ray structure of **78-12-2** had been determined. With this assumption, only two such addition patterns are possible for the C_{76}-$D_2(1)$ cage, and they are shown in Figure S-24 (Supporting Information). There are also three addition patterns with two symmetry-related p^2mp^2 ribbons, which are also shown in Figure S-24. All of these have unrealistically high relative energies. The addition pattern we tentatively favor at this point, and which is also shown as the Schlegel diagram labeled **76-12-2** in Figure 1, is the C_2-p^3mp,p^3mp isomer that (i) has a DFT-predicted relative energy 9.6 kJ mol^{-1} lower than that of the other C_2-p^3mp,p^3mp isomer and (ii) correlates slightly better than the other isomer with the ^{19}F NMR parameters. For example, the DFT F−C−C−C torsion angles for the CF_3 groups that give rise to multiplets **a** and **b** at $-\delta$ 56.8 and 60.2, respectively, are 23.4° and 27.5°, respectively, for the proposed isomer and are 52.2° and 10.9°,

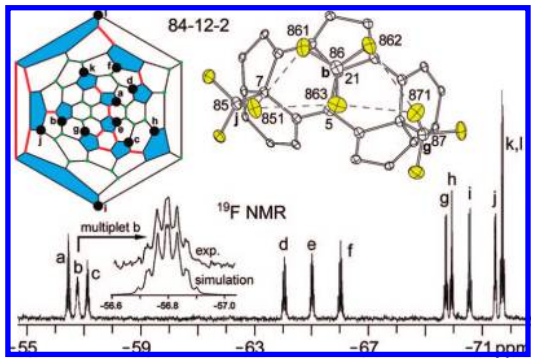

Figure 11. Schlegel diagram and 376.5 MHz ^{19}F NMR spectrum of **84-12-2** (C_1-p^6,p^2,p-(C_{84}-C_2(11))(CF_3)$_{12}$. An expansion of multiplet **b** and a spectral simulation with J_{FF} values of 11 and 15 Hz are shown. A fragment of the X-ray structure of **84-12-2** (see ref 18) that shows the eclipsed nature of the C86 CF_3 group, which gives rise to multiplet **b**, is displayed at the top. The F863−C86−C21−C5 torsion angle, which defines the conformation of the CF_3 group with respect the fullerene cage, is 14.1(1)°. The F851···F861, F851···F863, F862···F871, and F863···F871 distances are 2.678(2), 2.906(2), 2.702(2), and 2.648(2) Å, respectively.

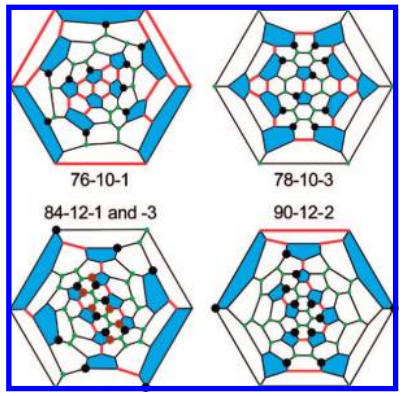

Figure 12. Color-coded Schlegel diagrams for the proposed structures of **76-10-1**, **78-10-3**, **84-12-1** and **-3**, and **90-12-2**. The 12 pentagons in each Schlegel diagram are highlighted in blue, the interpentagonal C−C bonds (ICCBs) are highlighted in red, and THJs are represented as small green circles. In all cases, large black circles represent cage C(sp^3) atoms. In the Schlegel diagram for **84-12-1** and **-3**, the black circles are the **84-12-1** addition pattern (overall D_2 symmetry) and the outer black circles and the inner brown circles are the **84-12-3** addition pattern (overall C_2 symmetry).

respectively, for the second isomer (see Table 3). A torsion angle of 52.2° is not consistent with a $-\delta$ value below 60.

4. Addition Pattern of 76-6-1. The NMR spectrum of this compound consists of two quartets, two quartets-of-quartets, and two unresolved multiplets, indicating C_1 symmetry and suggesting a single ribbon of five edge-sharing $C_6(CF_3)_2$ hexagons. Even though a C_2-p^5,p^5 addition pattern is not possible for (C_{76}-D_2(1))(CF_3)$_{12}$, one, and only one, single-ribbon C_1-p^5 addition pattern is possible for the composition (C_{76}-D_2)(CF_3)$_6$, and it is by far the most stable (by 30 kJ mol^{-1}) and therefore the most likely addition pattern for **76-6-1**. It is shown in Figure S-25 (Supporting Information) along with the seven other single-ribbon addition patterns that use *p*- and *m*-$C_6(CF_3)_2$ hexagons and avoid sp^3 THJs. The proposed addition pattern also has the highest DFT-predicted HOMO−LUMO gap, 1.560 eV.

5. Addition Patterns of 76-8-1 and -2. The NMR spectra of these two compounds are both consistent with a C_1-p^5,p, C_1-p^3mp,p, or C_1-*pmpmp*,*p* addition pattern. Because of the asymmetric nature of these molecules, there are many possible isomers to consider. We chose as starting points the four lowest-energy single-ribbon addition patterns discovered for the composition (C_{76}-D_2(1))(CF_3)$_6$. We further limited our computational study to those isomers without sp^3 THJs, and 58 such isomers are shown in Figure S-26 (Supporting Information) along with their DFT-predicted relative energies and HOMO−LUMO gaps. We then compared the DFT-optimized structural parameters with the NMR data for the 10 isomers with DFT-predicted relative energies of 0.0−22.9 kJ mol^{-1} (eight are C_1-p^5,p isomers and two are C_1-p^3mp,p isomers). The fact that neither **76-8-1** nor **76-8-2** has a multiplet with a $-\delta$ value significantly below 60 suggests that their structures should not have any CF_3 groups with F−C−C−C torsion angles significantly below 20°. Furthermore, the $^7J_{FF}$ values of 8 and 15 Hz for the CF_3 groups for the isolated *p*-$C_6(CF_3)_2$ hexagons and of ca. 17 Hz for both terminal CF_3 groups in both compounds place limitations on what the relevant F···F distances can be. On the basis of these comparisons and considering their relative energies, which are listed in Table S-5 (Supporting Information), we tentatively assign **76-8-1** and **76-8-2** to the addition patterns shown as Schlegel diagrams in Figure 1 (note that both are p^5,p addition patterns). Their IUPAC lowest locants and HOMO−LUMO gaps are listed in Table 1.

6. Possible Types of Addition Patterns for 76-10-2, -3, -4, and -5. The ^{19}F NMR spectra of all four of these asymmetric compounds consist of four quartets-of-quartets (in some cases these are unresolved multiplets) and six quartets. In the case of **76-10-4**, none of the quartet J_{FF} values are the same. Therefore, this compound has two ribbons of three CF_3 groups and one ribbon of four CF_4 groups. The other three compounds have a ribbon of six CF_3 groups (presumably a p^3mp or a *pmpmp* ribbon) and two isolated *p*-$C_6(CF_3)_2$ hexagons. An analysis of the NMR and DFT-predicted structural parameters, similar to the one that was performed for **76-8-1** and **76-8-2**, is shown in Table S-6 (Supporting Information; see also Figure S-25), and tentative assignments for **76-10-2**, **-3**, and **-5** are listed as IUPAC lowest locants in Table 1. In general, the agreement between the NMR and structural parameters is not as good for these three $C_{76}(CF_3)_{10}$ derivatives as it is for **76-8-1** and **76-8-2**.

7. Addition Pattern of 78-8-1. The ^{19}F NMR spectrum of this compound consists of four multiplets, one quartet, and three quartet-of-quartets. This is consistent with a single ribbon and overall C_s or C_2 symmetry. Only five isomers are possible if THJs are avoided for the three known soluble cages, C_{78}-D_3(1), C_{78}-C_{2v}(2), and C_{78}-C_{2v}(3), and these are shown in Figure S-26. The lowest energy structure, with a HOMO−LUMO gap of 1.907 eV, is the structure that is most consistent with the NMR data (see Table 3), and we believe that this is the most likely structure of **78-8-1**. Note that it is also the only *para*-only addition pattern among the five potential isomers. The IUPAC lowest locants and a Schlegel diagram for the proposed structure molecule are given in Table 1 and Figure 1, and a θ_p plot is shown in Figure S-15.

8. Addition Pattern of 78-10-3. We noted in the X-ray structure section that there is a second *para*-only isomer possible for a (C_{78}-C_{2v}(2))(CF_3)$_{10}$ isomer with C_2 or C_s symmetry (the first such isomer is the C_s-p^7 structure of **78-10-2**). It is a C_2-p^4,p^4 addition pattern, and its DFT-predicted relative energy is only 20 kJ higher than that of **78-10-2**. It is shown as the Schlegel diagram labeled **78-10-3** in Figure 1. Interestingly, the θ_p plot for the proposed structure is identical to the θ_p plot for **78-10-2** shown in Figure 9. In fact, the Schlegel diagram for **78-10-3** differs from the **78-10-2** Schlegel diagram in Figure 9

by moving one CF_3 group from C72 to C74. Two aspects of the DFT-optimized proposed structure for **78-10-3** correlate well with the ^{19}F NMR parameters. First, the sequence of $-\delta$ values 57.4, 59.4, 60.9, 66.8, and 70.0 have DFT-predicted F−C−C−C torsion angles of 21.9°, 21.7°, 32.3°, 47.3°, and 54.2°. Second, the J_{FF} value of 11.3 Hz for quartet **e** correlates well with the predicted F···F distance of 2.711 Å.

However, there is a feature of the ^{19}F NMR spectrum of **78-10-3** that we have not encountered in the spectra of more than 75 fullerene$(CF_3)_n$ compounds we have examined up until now. According to the proposed addition pattern, there should be two quartets because there are two different terminal CF_3 groups on each p^4 ribbon. Therefore, multiplet **d** should be assigned to a terminal CF_3 group, along with quartet **e**. However, multiplet **d** is clearly not a quartet: although it is unresolved, its vertical intensity is significantly less than that of quartet **e**, as shown in Figure S-28 (Supporting Information). Since the *overall* width of multiplet **d** is smaller, not larger, than the overall width of quartet **e**, this requires that the CF_3 group on each ribbon that gives rise to multiplet **d** must be coupled to *two* CF_3 groups, not just one (i.e., multiplet **d** must be composed of more individual resonances that quartet **e**). However, the 2D COSY NMR spectrum of **78-10-3**, which is shown in Figure S-29 (Supporting Information) along with the 2D spectrum of **78-10-2** for comparison, indicates that each multiplet **d** CF_3 group is coupled to a multiplet **c** CF_3 group but is not coupled to the other three CF_3 groups. In fact, the two 2D spectra are homologous with respect to the 2D correlations, and the chemical shifts are similar as well. Therefore, we must conclude that the addition patterns of **78-10-2** and **78-10-3** are very similar and that the multiplet **d** CF_3 groups in **78-10-3** are coupled to one another (in addition to being coupled to different multiplet **c** CF_3 groups), even though the multiplet **d** CF_3 groups in **78-10-3** *do not* share a common hexagon like the multiplet **d** CF_3 groups in the single-ribbon isomer **78-10-2**. Although the multiplet **d** CF_3 groups in **78-10-3** are isochronous, they are not magnetically equivalent, and their mutual coupling can affect the splitting pattern, and hence the vertical intensity, of the multiplet.

The two multiplet **d** *terminal* CF_3 groups in the proposed structure are bonded to C(sp^3) atoms that are separated from one another by only two C(sp^2) atoms, as shown in Figure 13. The F atoms of these CF_3 groups are separated by seven F−C and C−C bonds, as are the F atoms in the two CF_3 groups in any fullerene *p*-$C_6(CF_3)_2$ hexagon. However, unlike the F atoms on different CF_3 groups in a *p*-$C_6(CF_3)_2$ hexagon, which can approach one another to within 2.5−3.0 Å and experience significant "through-space" $^7J_{FF}$ coupling of up to 180 Hz (the observed coupling is one-ninth of this value due to rapid rotation of the CF_3 groups) via F atom lone pair-lone pair overlap,[7] the closest approach of the F atoms on the C83 and C84 CF_3 groups in the DFT-optimized structure of **78-10-3** is 4.08 Å for F832···F841, as shown in Figure 13. This is too long a distance for observable through-space J_{FF} coupling of even a few hertz.[64−66] ["Through-space J_{FF} coupling", although a misnomer because it is more generally used to describe the dipolar spin−spin coupling mechanism that is not observable in liquid NMR because dipolar coupling is averaged to zero, is a term that has been used by NMR spectroscopists since the 1960s[67] to describe J_{FF} coupling due to direct lone pair−lone pair interactions between, for example, proximate F atoms (i.e., a more definitive terminology frequently used is "through-space" Fermi-contact coupling).[64−66]]

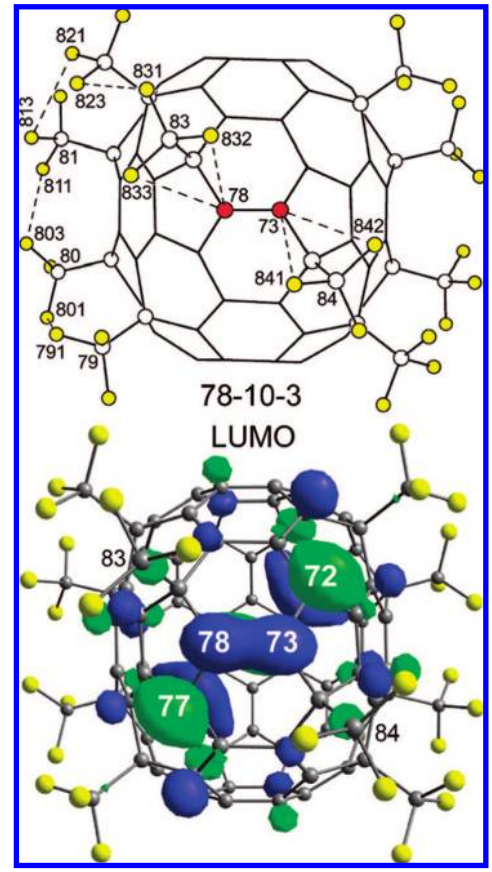

Figure 13. Drawings of the DFT-optimized structure and LUMO of C_2-(C_{78}-C_{2v}(2))$(CF_3)_{10}$ (**78-10-3**). The blue (+) and green (−) regions represent the lobes of the π atomic orbitals for each C atom scaled according to their contributions to the LUMO. Note that C83 and C84 contribute to the LUMO to a much greater extent than do the other CF_3 C atoms. It is proposed that through-space Fermi-contact coupling between the ^{19}F nuclei on the C83 and C84 CF_3 groups is due, in part, to overlap of the F atom lone pairs of electrons with the LUMO π orbital lobes on C77 and C78. The DFT-predicted F832···C78 and F833···C78 distances are 2.755 and 2.932 Å, respectively.

If the proposed structure of **78-10-3** and our interpretation of the vertical intensity of multiplet **d** are correct, it would represent the first example of a fullerene$(CF_3)_n$ derivative in which the *effect* of J_{FF} coupling (although not a measureable splitting itself) has been observed between CF_3 groups that do not share the same hexagon or pentagon. One possible explanation for this phenomenon is that the C83 and C84 CF_3 groups are J_{FF} coupled via overlap of the F832 and F841 lone-pair electrons with the LUMO of **78-10-3**, which has significant orbital contributions from C73 and C78, as also shown in Figure 13. Note that C83 and C84 also contribute to the LUMO more so than do the other CF_3 C atoms. However, other coupling pathways involving other molecular orbitals are possible, and we cannot rule out any of them at this time. (It is also possible that the proposed structure of **78-10-3** is incorrect.) We intend to study this phenomenon in more detail in the future, both experimentally and computationally, including the structure elucidation of **78-10-3** by X-ray crystallography once suitable crystals have been grown.

9. Addition Pattern of 78-12-2 and Possible Types of Addition Patterns for 78-14-1. The 2D COSY ^{19}F NMR spectrum of **78-12-2** is shown in Figure S-30 (Supporting

(64) Ernst, L.; Ibrom, K. *Angew. Chem., Int. Ed.* **1995**, *34*, 1881–1882.
(65) Alkorta, I.; Elguero, J. E. *Struct. Chem.* **2004**, *15*, 117–120.

Information) along with drawings showing the eclipsed nature of the multiplet **b** CF_3 group and the simulation of one of the multiplets showing that it is a quartet-of-quartets. The ^{19}F NMR spectrum of **78-14-1** consists of 14 multiplets, 4 quartets, and 10 multiplets. The 2D COSY spectrum, shown in Figure S-31 (Supporting Information), clearly demonstrates that the addition pattern has a ribbon of 11 CF_3 groups and a ribbon of 3 CF_3 groups. It is clear that **78-14-1** is not simply the product of **78-12-2** and two additional CF_3 groups. At this time, it is not even possible to narrow down the C_{78} cage isomer of **78-14-1** or to determine any other feature of its addition pattern.

10. Addition Patterns of 84-12-1 and -3. The ^{19}F NMR spectrum of **84-12-1** is distinctive in that it consists of only three multiplets, a quartet, and two unresolved multiplets (presumably quartets-of-quartets), requiring two ribbons of six CF_3 groups and overall D_2, C_{2v}, or C_{2h} symmetry, all of which are subgroups of the D_2, D_{2d}, and/or D_{6h} point groups. The low-abundance C_{84}-D_{6h}(24) cage can be eliminated because **84-12-1** is the most abundant isomer of this composition. Furthermore, the C_{84}-D_{2d}(23) cage can be eliminated because the two required ribbons, which must be p^5 or, less likely, *pmpmp* and must each be two-fold symmetric in addition to being symmetry-related to each other, are not possible for this cage. That leaves the C_{84}-D_2(22) cage as the only abundant C_{84} cage possible for **84-12-1**, and there are four possible two-ribbon isomers with the required overall D_2 symmetry. One of these involves sp^3 THJs and can be eliminated from consideration on this basis. The other three were optimized by DFT. One of them, the one we believe is the most likely for **84-12-1**, is more than 43 kJ mol^{-1} more stable than the other two (and the other two have unreasonably small HOMO−LUMO gaps of less than 1 eV). Therefore, the D_2-p^5,p^5-(C_{84}-D_2(22))$(CF_3)_{12}$ addition pattern shown as a Schlegel diagram in Figures 1 and 12 almost certainly represents the structure of **84-12-1**. The excellent fit of its DFT-optimized structure and its ^{19}F NMR spectrum is shown in Table 3. The ^{19}F NMR spectrum of **84-12-3** consists of six multiplets, two of which are quartets and three of which (including one of the quartets) are almost identical in chemical shift and multiplet structure to the three multiplets of **84-12-1** (see Table 3). Furthermore, the C_{84}-D_2(22) addition pattern shown in Figures 1 and 12 for **84-12-3**, which has the required overall C_2 symmetry, is the only possible addition pattern for any of the nine C_{84} cages that are known. Therefore, the C_2-p^5,p^5-(C_{84}-D_2(22))$(CF_3)_{12}$ addition pattern shown in Figures 1 and 12 almost certainly represents the structure of **84-12-3**. The proposed structures of **84-12-1** and **84-12-3** follow the new addition-pattern principle discussed above for all other *para*-only $HFF(CF_3)_n$ structures, as shown in Figure S-20.

11. Fluorine-19 NMR Spectra of 84-10-1 and 84-14-1. The ^{19}F NMR $-\delta$ and J_{FF} values for these compounds are listed in Table 4. Both compounds are asymmetric, and it is not possible at this time to say much about their addition patterns except that **84-10-1** probably has an addition pattern with either two ribbons or a loop of six $C_6(CF_3)_2$ hexagons and/or $C_5(CF_3)_2$ pentagons plus two isolated *p*-$C_6(CF_3)_2$ hexagons (the terminal quartet J_{FF} values are too similar to distinguish between these two possibilities) and that **84-14-1** probably has an addition pattern with two ribbons. It is likely that one or both of these compounds contain the C_{84}-D_{2d}(23) cage, since this abundant cage is not represented in the other three $C_{84}(CF_3)_n$ compounds isolated in this work.

12. Addition Pattern of 90-12-2 and Types of Addition Patterns for 90-12-1. The ^{19}F NMR spectrum of **90-12-2** consists of 12 multiplets, six of which are quartets, requiring overall C_1 symmetry. The J_{FF} values and second-order nature of two pairs of the quartets require that the structure of this molecule has an $8 + 2 + 2$ addition pattern. We will assume that the most likely type of addition pattern for **90-12-2** would be C_1-p^7,*p*,*p*. There are 46 possible IPR C_{90} fullerenes,[16] and the ones that are predicted to be reasonably stable, both thermodynamically and kinetically, are C_{90}-D_{5h}(1), C_{90}-C_1(27), C_{90}-C_2(28), C_{90}-C_1(29), C_{90}-C_1(30), C_{90}-C_2(31), C_{90}-C_1(32), C_{90}-C_s(34), C_{90}-C_s(35), C_{90}-C_2(40), C_{90}-C_2(45), and C_{90}-C_{2v}(46).[68,69] Of these, C_1-p^7,*p*,*p* ribbons are only possible on the C_{90}-C_1(27), C_{90}-C_2(31), C_{90}-C_1(32), and C_{90}-C_2(45) cages. The 13 C_1-p^7,*p*,*p* addition patterns for these four cages are listed in Table S-7 (Supporting Information). Given the DFT-predicted relative energies and HOMO−LUMO gaps, only one of these is a reasonable choice for **90-12-2**, and that is the one shown as a Schlegel diagram in Figures 1 and 12 and for which the IUPAC lowest locants and DFT-predicted HOMO−LUMO gap are listed in Table 1. The data in Table 3 show that the DFT-optimized structure correlates extremely well with the ^{19}F NMR spectrum of **90-12-2**. For example, the multiplet at δ −53.8 is assigned to a CF_3 group that is nearly eclipsed (its F−C−C−C torsion angle is 8.8°), and the F···F distances for the two isolated *p*-$C_6(CF_3)_2$ hexagons, at 2.738 and 2.893 Å, fit the J_{FF} values for these quartets, 11 and 6 Hz, respectively. In contrast, the only other C_1-p^7,*p*,*p* addition pattern within 36 kJ mol^{-1} of the proposed structure has isolated *p*-$C_6(CF_3)_2$-hexagon F···F distances of 2.586 and 2.595 Å, far too short for the observed J_{FF} values. The compound **90-12-2** is the best example of the ability of ^{19}F NMR spectroscopy combined with DFT calculations of addition patterns consistent with the principles (i.e., general trends, not hard-and-fast rules) we have discovered for $HHF(CF_3)_n$ compounds, to narrow down the possible addition patterns to one "most likely" structure.

It is not possible to narrow down the possible addition patterns for **90-12-1**, the ^{19}F NMR spectrum of which consists of eight quartets and only four quartets-of-quartets, as shown in Figure 4 and Table 4. The addition pattern clearly has overall C_1 symmetry, two isolated *p*-$C_6(CF_3)_2$ hexagons, and two ribbons, which could be ribbons of three and five CF_3 groups or four and four CF_3 groups. There are too many possibilities to consider at this time. Nevertheless, we predict that this compound will have three CF_3 groups that are nearly eclipsed, and this would make ribbons of three and five CF_3 groups more likely than two ribbons of four CF_3 groups. This is because no well-characterized fullerene$(CF_3)_n$ compound has yet been found to have two nearly eclipsed CF_3 groups that share the same $C_6(CF_3)_2$ hexagon.

Conclusions

Twenty-one new fullerene$(CF_3)_n$ compounds with the C_{76}-D_2(1), C_{78}-D_3(1), C_{78}-C_{2v}(2), C_{78}-C_{2v}(3), C_{84}-C_2(11), C_{84}-D_2(22), C_{90}-C_1(32), and possibly several other hollow-higher-fullerene (HHF) cages have been isolated and characterized, bringing the total number of known $HHF(CF_3)_n$ compounds to 28. An

(66) Arnold, W. D.; Mao, J.; Sun, H.; Oldfield, E. *J. Am. Chem. Soc.* **2000**, *122*, 12164–12168.
(67) Petrakis, L.; Sederholm, C. H. *J. Chem. Phys.* **1961**, *35*, 1243–1248.
(68) Sun, G. *Chem. Phys.* **2003**, *289*, 371–380.
(69) Watanabe, M.; Ishimaru, D.; Mizorogi, N.; Kiuchi, M.; Aihara, J. *J. Mol. Struct. (Theochem)* **2005**, *726*, 11–16.

analysis of the addition patterns of these compounds and three other $HHF(X)_n$ compounds with bulky X groups has led to the discovery of the following addition-pattern principle for HHFs: In general, the most pyramidal cage $C(sp^2)$ atoms in the parent HHF, which form the most electron-rich and therefore the most reactive cage C−C bonds as far as 1,2-additions are concerned, are not the cage C atoms to which bulky substituents are added. Instead, ribbons of edge-sharing p-$C_6(X)_2$ hexagons, with X groups on less pyramidal cage C atoms, are formed, and the otherwise "most reactive" fullerene double bonds remain intact.

Acknowledgment. The authors express their gratitude to Manfred Kappes for his encouragement and support and to Carlo Thilgen and Warren Powell for assistance with fullerene nomenclature and numbering. This work was supported by the U.S. National Science Foundation (CHE-0707223), the Civilian Research and Development Foundation (RUC2-2830-MO-06), the AvH Foundation, the Volkswagen Foundation (I-77/855), the DAAD, the Fonds der Chemischen Industrie (Germany), the Russian Foundation for Basic Research (06-03033147-a), the Russian Science Support Foundation, the Moscow State University Research Computing Center, and the Colorado State University Research Foundation.

Note Added in Proof. The structure of an isomer of $C_{78}Cl_{18}$ was recently determined and was reported to contain the previously unobserved C_{78}-D_{3h}(4) cage.[70] However, this report is in error; the compound reported is a derivative of the known C_{78}-D_{3h}(5) cage.

Supporting Information Available: Crystallographic data in CIF format and additional figures and tables. This material is available free of charge via the Internet at http://pubs.acs.org.

JA8041614

(70) Simeonov, K. S.; Amsharov, K. Y.; Krokos, E.; Jansen, M. *Angrew. Chem., Int. Ed.* **2008**, *47*, 6283–6285.